"Transient Performance of Variable-Reluctance Stepping Motors"

A Thesis

Presented To

The Faculty of Graduate Studies

The University of Manitoba

In partial fulfillment

of the requirements for the degree of

MASTER OF SCIENCE

IN

ELECTRICAL ENGINEERING

By

RAVINDER KUMAR GUPTA

MAY, 1975

"TRANSIENT PERFORMANCE OF

VARIABLE-RELUCTANCE STEPPING MOTORS"

by

RAVINDER KUMAR GUPTA

A dissertation submitted to the Faculty of Graduate Studies of the University of Manitoba in partial fulfillment of the requirements of the degree of

MASTER OF SCIENCE

ABSTRACT

Multistep operation of a stepping motor can be quite different from single step operation. This thesis presents a study of the ultimate performance limitations, of a stepping motor when supplied by a series of pulses for multiple stepping and for single step operation. The results have been obtained by simulation studies on Analog and Digital Computers. The effects of machine and load parameters on the limiting performance have been obtained which should prove valuable both for the designers of stepping motors and application engineers.

ACKNOWLEDGEMENT

The author would like to express his appreciation and deepest gratitude to Professor R.M. MATHUR for suggesting the thesis topic, his esteemed guidance in the preparation of this thesis, and financial support.

TABLE OF CONTENTS

LIST OF ILLUSTRATIONS

LIST OF SYMBOLS

Main Symbols

i	instantaneous current, A.
J	moment of inertia of the system, $Kg\text{-}m^2$
K	number of pulses per second, p.p.s.
K_1	damping coefficient, N-m-s/rad
K_2	stiffness coefficient, N-m/rad.
L	self inductance of stator windings, H.
L_{max}	maximum self inductance, H.
L_{min}	minimum self inductance, H.
L_v	variable part of the inductance, H.
P	number of stator phases
R	resistance of each stator winding, Ω.
t	time, S.
T	number of teeth in each stator phase or rotor.
T_a	approximated equivalent time constant, s.
T_L	load torque, N-m.
TR	resultant motor torque, N-m.
V	instantaneous voltage, V.
V_{max}	maximum voltage, V.
w	width of each pulse, s.
θ	instantaneous position, rad.
θ_s	step angle, rad.

Subscripts

A,B,C,1,2,P.	stator phases
SS,MS,OUT	single-step, multiple-step, pull-out

CHAPTER 1

INTRODUCTION

In recent years the use of pulse technology in the field of automatic control has rapidly increased. In fact, the digital control of the tooling machines is being used intensively and the number of tooling machines not employing digital control is continuously declining.

A stepping motor is basically a D-A convertor since it is capable of rotating through a predetermined angle with the application of prescribed number of electrical pulses. The input is usually in the form of rectangular voltage pulses. The rotational angle and the angular velocity of rotation depends, respectively, upon the pulses fed and the pulse rate (p.p.s.)

Basically, there are two types of stepping motors.

(i) Variable-reluctance stepping motors,

and (ii) Permanent-magnet stepping motors.

The variable-reluctance stepping motors usually consist of three or more phases. The stator windings are housed on salient poles which form electromagnetic structures on excitation. When one or more stator windings are excited or energized, the rotor takes a position to provide a path of minimum reluctance for the magnetic flux. When the windings in the stator are energized one after another, in a particular sequence, a continuous motion takes place. Excitation of more than one winding, sequentially, may be adopted to obtain a smaller step angle.

A permanent-magnet stepping motor consists of a permanent magnet rotor. The stator windings are wound on salient poles, as in a variable reluctance machine. When any one of the stator windings is energized,

the interaction between the magnetic flux set up by a stator coil and the permanent magnet rotor produces torque causing the rotor to move in such a way that the magnetic moment of the permanent magnet aligns with the stator winding magnetic field.

A number of papers have been published on the operation and analysis of stepping motors. The published work suffers from one drawback or another owing to the simplistic assumptions made by the authors and hence, a need exists to analyse the dynamic performance of a stepping motor under transient conditions and to obtain the limits of satisfactory operation by simple analytical expressions. The study undertaken in this thesis is aimed to bridge this gap. O'Donahue[1] has developed a linear second-order transfer function for the analysis and approximately describes the dynamics of the stepping motor for a single step operation, which is unsuitable for the multi-step operation Kuo, Singh and Yackel[2] have approximated the inductance waveforms, for a particular motor, as the function of rotor position. Their treatment lacks generality. Also, the adjustment of a particular constant in the torque equation just to make the practical results match with the theoretical results seems arbitrary, since its validity has neither been explained nor mentioned. Venkataratnam, Sarkar and Palani[3] have neglected inductance in comparison with the resistance of the stator windings. This is equivalent to assuming constant currents in the stator windings. But how far they have been able to achieve this ideal current source practically has not been indicated. The load-torque has also been neglected in comparison with inertial and frictional torques. Robinson and Taft[4] have also done the analysis assuming the constant current source. Venkataratnam and Mouli[5] have replaced the rectangular voltage with the sinusoidal input for the

convenience of analytical treatment

The purpose of this thesis is to develop the models, both analog and digital, to suit the performance of a variable-reluctance, (VR) stepping motor. In Chapter II, both analog and digital models for a simple three-phase motor and a general digital-model for a P-phase motor are developed. Because of the limitations of components available on the analog computer, the response simulated is primarily for a single pulse. However, the simulated results serve to predict the motor performance, when the last pulse is applied continuously to hold the rotor at a desired position, to eliminate the requirement of detenting windings, after having achieved the incremental motion as desired, by supplying a series of pulses or one pulse at a time, depending upon the number of phases and number of teeth present and the angle of rotation required. The schematic diagram, for simulating the multi-step operation of the VR stepping motor is given in Fig. 2.2.2. The motor is simulated first by using Fourier series for both voltage and inductance waveforms, second, by generating exact voltage waveforms in Fourier series and finally, by generating the exact waveforms both for voltages and inductances of an idealized motor. Depending upon the shape of the supply voltage and inductance waveforms of a particular motor, dependent on the shape of the rotor slots and stator pole shape, one of the above computer programs may be used to economize the computational time.

In addition to the development of the above simulation techniques, in Chapter III expressions for an absolute upper limit of frequency, the maximum pull-in frequency as applicable to single-step operation and multiple-stepping and for the pull-out frequency in terms of load torque,

inertia and damping are derived. The operational performance is discussed in Chapter IV.

Safe pull-in frequency in combination with the pull-out frequency may be used as the performance criterion for the selection of a motor for a particular application.

Self-inductance versus position curve, experimentally determined for a particular motor, is given in Appendix 3 in support of the theoretical model.

CHAPTER 2

ANALYSIS OF THE VARIABLE RELUCTANCE STEPPING MOTOR

2.1. The analysis of a simple three phase VR stepping motor

The type of motors being analyzed here have the following specific features, detailed briefly with their operation.

(i) Each unit is identical in construction to others and a P-phase motor can easily be assembled by putting P-modular units together. All the rotors are aligned along the rotor axis. However, poles of the stators of phase A, phase B and phase C are mis-aligned by 360/PxT degrees. Each rotor has as many teeth (T) as a stator.

(ii) Torque may be increased by having more than one unit per phase.

(iii) Highest stepping rate can be achieved by using thin discs solidly attached to the shaft instead of using conventional rotors, because of the low inertia.

To briefly explain the principle of operation of a VR motor, assume the rotor of phase A to be in a position of minimum reluctance, as shown by solid lines in Fig. 2.1.1. When the phase B is excited, the motor moves one step angle in a clockwise direction to provide a path a minimum reluctance for the magnetic flux of B. If the stator coils are excited in sequence A→B→C, the motor would move clockwise executing one step angle by excitation of one phase. It may be rotated in anti-clockwise direction by exciting the phases A→C→B, with the same step. Smaller step angles may be obtained by energization sequence of A→AB→B→BC→C→CA or A→AC→C→CB→B→BA depending upon the direction one wants the motor to move.

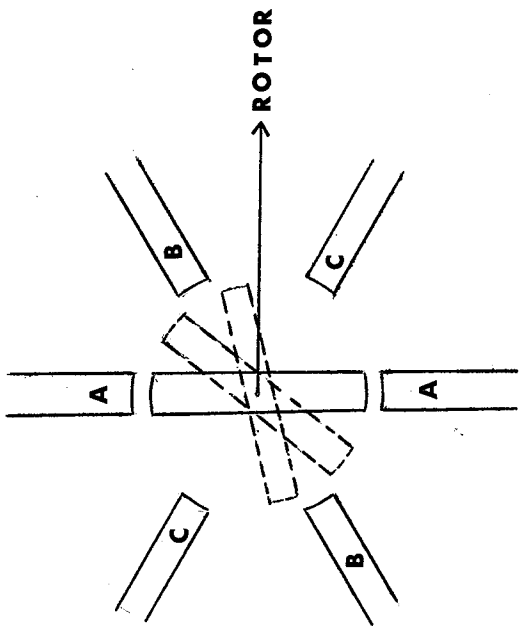

Fig.2.1.1. THREE-PHASE TWO-POLE MACHINE

The assumptions made for the analysis are:

(i) Inductances of the stator windings are functions of rotor position (θ) only. This is equivalent to assuming that no saturation occurs and flux linkages are directly proportional to the exciting currents. The inductance waveforms are at first approximated by triangular waveforms.

(ii) The voltage input pulses are of rectangular shape (which is usually the case).

(iii) On account of the nature of machines being analyzed, no mutual coupling exists between coils of different phases. This assumption is reasonable even for a single stator machine so long as only one coil is excited at one time.

(iv) The overall shape and magnitudes of inductances of all coils are identical. This assumption results from the identical geometry of all units of a multi-stack machine.

The above waveforms are approximated by the Fourier series to allow a generality in the analysis which would permit adequate representation of non-rectangular voltage pulses and non-triangular inductance waveforms, by including an appropriate number of harmonics for predicting the dynamic response.

The inductance and voltage waveforms for the above motor are drawn in Figs. 2.1.2 and 2.1.3.

Since these waveforms are periodic and satisfy the Dirichlet's conditions that they are continuous except for a possibility of finite number of maxima and minima, they can be represented by infinite series.

As derived in appendix (1), the inductance and voltage waveforms for phases A, B and C are:

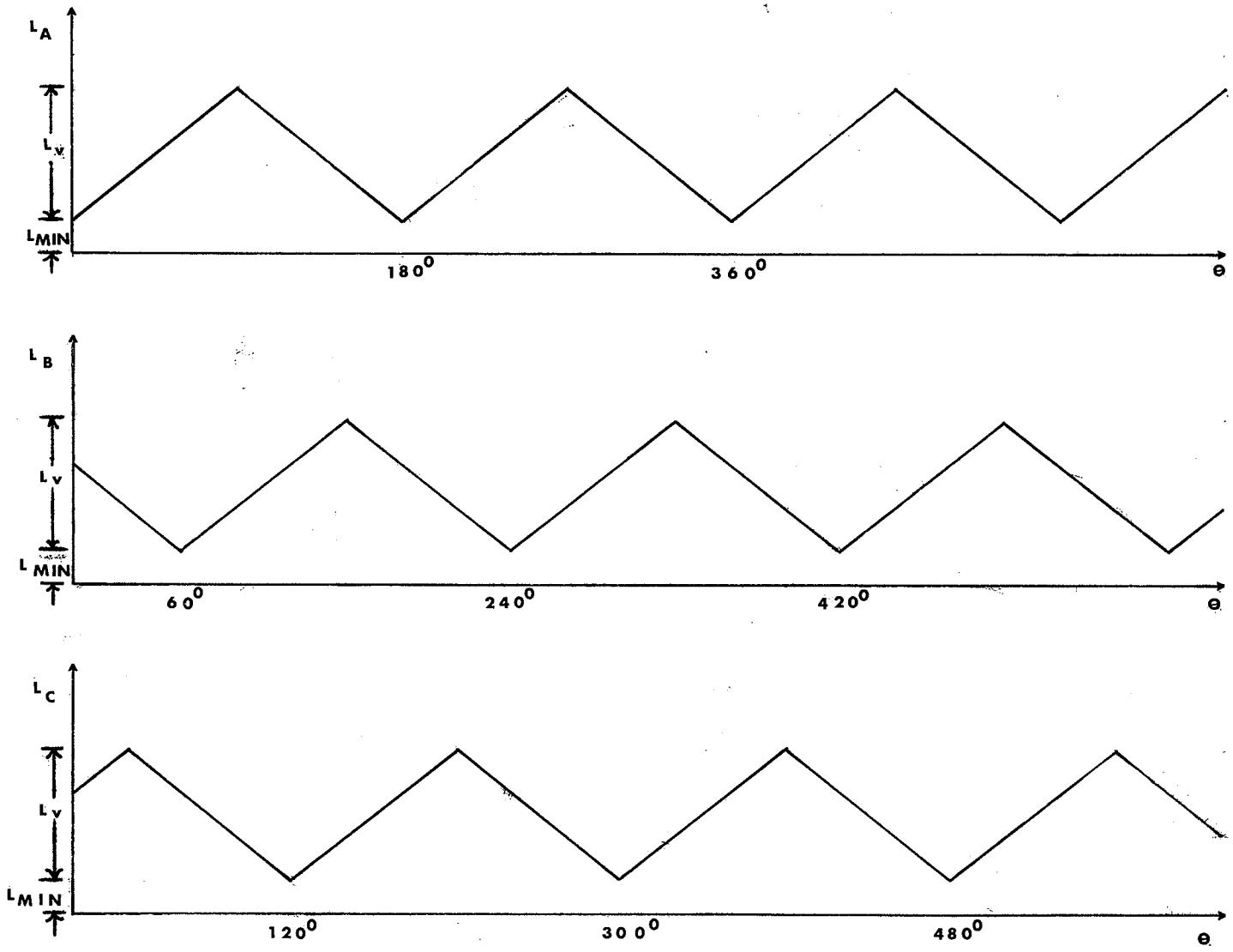

Fig.2.1.2. INDUCTANCE WAVEFORMS FOR A TWO-POLE THREE-PHASE MACHINE

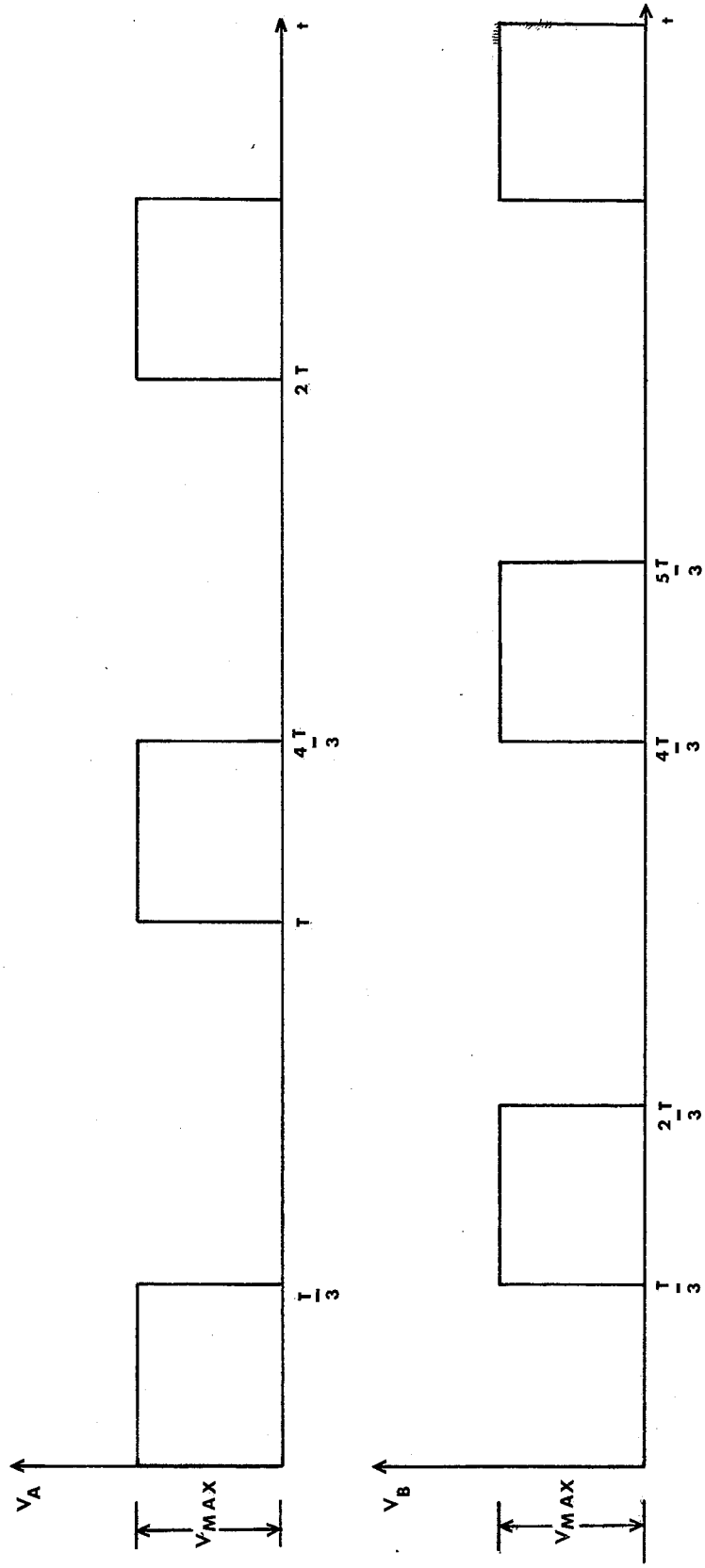

Fig.2.1.3. VOLTAGE WAVEFORMS FOR A THREE-PHASE MACHINE

$$L_A(\theta) = L_{min} + \frac{L_v}{2} + \frac{2L_v}{\pi^2} \sum_{n=1}^{\infty} \frac{1}{n^2} \left[(-1)^n - 1 \right] \cos(2n\theta) \quad \text{.....2.1.1.}$$

$$L_B(\theta) = L_{min} + \frac{L_v}{2} + \frac{2L_v}{\pi^2} \sum_{n=1}^{\infty} \frac{1}{n^2} \left[(-1)^n - 1\right] \{\cos 2n(\theta - \pi/3)\} \text{.2.1.2.}$$

$$\text{and } L_C(\theta) = L_{min} + \frac{L_v}{2} + \frac{2L_v}{\pi^2} \sum_{n=1}^{\infty} \frac{1}{n^2} \left[(-1)^n - 1\right] \{\cos 2n(\theta - \frac{2\pi}{3})\} \text{.2.1.3}$$

Also,

$$V_A(t) = \frac{V_{max}}{3} + \frac{V_{max}}{\pi} \sum_{n=1}^{\infty} \left[\frac{1}{n} \sin(\frac{2n\pi}{3}) \cos(\frac{2n\pi t}{T}) + \frac{1}{n}(1-\cos\frac{2n\pi}{3}) \sin \frac{2n\pi t}{T} \right] \text{...2.1.4}$$

$$V_B(t) = \frac{V_{max}}{3} + \frac{V_{max}}{\pi} \sum_{n=1}^{\infty} \left[\frac{1}{n} \sin(\frac{2n\pi}{3}) \cos \frac{2n\pi(t-T/3)}{T} + \frac{1}{n}(1-\cos\frac{2n\pi}{3}) \sin \frac{2n\pi(t-T/3)}{T} \right]$$

....2.1.5

and

$$V_C(t) = \frac{V_{max}}{3} + \frac{V_{max}}{\pi} \sum_{n=1}^{\infty} \left[\frac{1}{n} \sin(\frac{2n\pi}{3}) \cos \frac{2n\pi(t-2T/3)}{T} + \frac{1}{n}(1-\cos\frac{2n\pi}{3}) \sin \frac{2n\pi(t-2T/3)}{T} \right]$$

....2.1.6

The voltage equation for any one stator coil is

$$V = i(t)\, R + L(\theta) \frac{di(t)}{dt} + i(t) \frac{dL(\theta)}{d\theta} \cdot \frac{d\theta(t)}{dt} \quad \text{..... 2.1.7}$$

$L(\theta) \frac{di(t)}{dt}$ is the transformer voltage and $i(t) \frac{dL(\theta)}{d\theta} \cdot \frac{d\theta(t)}{t}$ is the back e.m.f. acting in opposition to the applied voltage.

or $\quad V = i(t) \left[R + \frac{dL(\theta)}{d\theta} \cdot \frac{d\theta(t)}{dt} \right] + L(\theta) \frac{di(t)}{dt}$

let $\quad V = y, \; R + \frac{dL(\theta)}{d\theta} \cdot \frac{d\theta(t)}{dt} = R + \frac{dL}{dt} = A$ and $i = x$

$\therefore \quad y = Ax(t) + L(\theta) \frac{dx(t)}{dt}$

or $\quad y - Ax(t) = L(\theta) \frac{dx(t)}{dt}$

or $\quad \int \frac{1}{L(\theta)}\, dt = \int \frac{dx(t)}{y - Ax(t)}$

Assuming that during a small interval of time or the step of integration, θ does not change appreciably i.e., $L(\theta)$ remains constant and so does A.

$$\therefore \quad \frac{t}{L} = -\frac{1}{A} \log (y - Ax) + Z \qquad \ldots\ldots\ldots 2.1.8.$$

where Z is the constant of integration.

At $t = o$, $x(t) = o$

$$\therefore \quad Z = \frac{1}{A} \log (y)$$

Substituting back in equation 2.1.8,, we get

$$\frac{At}{L} = \log (y/(y - Ax))$$

or $$\frac{y}{y-Ax} = e^{At/L}$$

or $$x = \frac{y}{A}(1 - e^{-At/L})$$

Therefore, in terms of the original parameters, we have

$$i = \frac{V}{R + \frac{dL(\theta)}{d\theta} \cdot \frac{d\theta(t)}{dt}} \left[1 - e^{-(R + \frac{dL(\theta)}{d\theta} \cdot \frac{d\theta(t)}{dt})\, t/L} \right]$$

$\ldots\ldots\ldots 2.1.9.$

Torque of the motor can be represented by the sum of the torques of all the three independent phases

$$\therefore \quad TR = T_A + T_B + T_C$$

$$= \frac{1}{2} (i_A)^2 \frac{dL_A(\theta)}{d\theta} + \frac{1}{2} (i_B)^2 \frac{dL_B(\theta)}{d\theta} + \frac{1}{2} (i_C)^2 \frac{dL_C(\theta)}{d\theta}$$

$\ldots\ldots\ldots 2.1.10.$

$\frac{dL_A}{d\theta}(\theta)$, $\frac{dL_B}{d\theta}(\theta)$, and $\frac{dL_C}{d\theta}(\theta)$ can be obtained directly from the respective inductance equations, 2.1.1., 2.1.2. and 2.1.3., as follows:

$$\frac{dL_A(\theta)}{d\theta} = \frac{4L_v}{\pi^2} \sum_{n=1}^{\infty} \frac{1}{n} \left[1 - (-1)^n\right] \sin(2n\theta) \quad \ldots\ldots\ldots 2.1.11.$$

$$\frac{dL_B(\theta)}{d\theta} = \frac{4L_v}{\pi^2} \sum_{n=1}^{\infty} \frac{1}{n} \left[1 - (-1)^n\right] \sin 2n(\theta - \pi/3) \quad \ldots 2.1.12.$$

and $$\frac{dL_C(\theta)}{d\theta} = \frac{4L_v}{\pi^2} \sum_{n=1}^{\infty} \frac{1}{n} \left[1 - (-1)^n\right] \sin 2n(\theta - \frac{2\pi}{3}) \quad \ldots 2.1.13.$$

Instantaneous speed and position i.e., $\frac{d\theta(t)}{dt}$ and $\theta(t)$ is obtained by using the equation of motion:

$$TR = J\frac{d^2\theta}{dt^2} + K_1\frac{d\theta}{dt} + K_2\theta + T_L \qquad \ldots\ldots\ldots 2.1.14.$$

Values of $i_A(t)$, $i_B(t)$ and $i_C(t)$ can be obtained using equation 2.1.9. by substitution of the respective values of $\frac{dL(\theta)'s}{d\theta}$, $\frac{d\theta(t)}{dt}$, $L(\theta)'s$, and $v(t)'s$. Substitution of $i_A(t)$, $i_B(t)$, $i_C(t)$, $\frac{dL_A(\theta)}{d\theta}$, $\frac{dL_B(\theta)}{d\theta}$ and $\frac{dL_C(\theta)}{d\theta}$ in equation 2.1.10. results in the instantaneous torque.

The equations 2.1.1. - 2.1.14. describe the transient operation of a stepping motor for multiple-step or single-step operation for positional control.

The choice of the number of harmonics to be included for voltage and inductance waveforms depends upon the supply voltage and the shape and depth of the rotor slots respectively. Inclusion of first three or four harmonics for the inductance waveforms is usually good enough. However, if higher accuracy is desired, tests for measurements of inductance should be conducted at different rotor positions if the pertinent data is not available from the manufacturer, and the number of harmonics included should be such that the simulated inductance waveforms match as closely as possible the measured ones.

The results from simulation studies are discussed in Chapter 4.

2.2. Analog model for the motor

Analog simulation is undertaken to gain an insight into the effects of various load parameters because it is very easy to vary these parameters on an analog computer as compared to a digital computer. As indicated earlier electrically and magnetically the electrical circuits of the three phases are isolated and hence each phase has its independent set of governing equations. However, the torques of the three independent

phases add algebraically. A block diagram, for the prediction of the response of a variable reluctance stepping motor, when supplied by a series of pulses is shown in Fig. 2.2.2.

Because of the limited number of computing elements available on the analog computer, the actual simulation was done only for one step response. As the results obtained from the analog computer agree with the results obtained from the digital computer, for single step operation, it is logical to assume that analog model results will be comparable to the results obtained from the digital computer, when the motor is supplied with a series of pulses.

The actual simulation schematic diagram for single step operation is given in Fig. 2.2.1.

The two equations governing the dynamics of the motor are:

$$J\frac{d^2\theta}{dt^2} + K_1\frac{d\theta}{dt} + K_2\theta + T_L = TR$$

For the results in this thesis K_2 is neglected, hence above equation is rewritten as:

$$J\frac{d^2\theta}{dt^2} + K_1\frac{d\theta}{dt} + T_L = TR \qquad \ldots\ldots\ldots 2.2.1.$$

Also, $$V = iR + L\frac{di}{dt} + i\frac{dL}{d\theta}\cdot\frac{d\theta}{dt} \qquad \ldots\ldots\ldots 2.2.2.$$

SCALING: The scaling procedure for the analog simulation is illustrated by one example.

TIME SCALING: Consider a case, when 100 p.p.s. are supplied. Therefore, duration of one pulse $= \frac{1}{100} = 0.01$ sec. $= w$. This is the real time. If T represents the computer time and h the time scale factor

$\therefore \quad t = \frac{T}{h}$

Choosing $h = 100$, $T = th = 0.01 \times 100 = 1$ sec.

Substituting $t = \frac{T}{h}$ in equations 2.2.1., and 2.2.2., we get

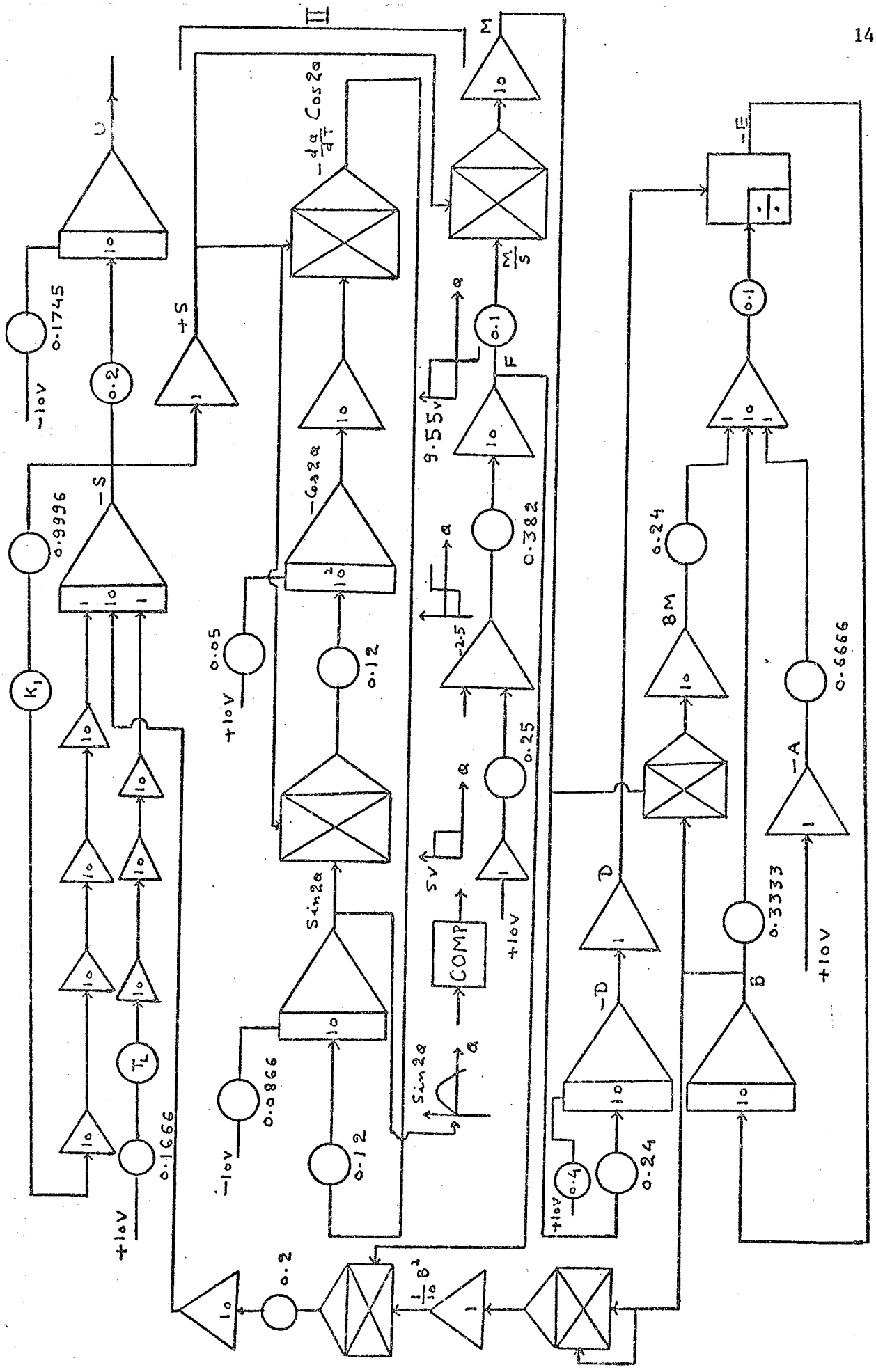

Fig.2.2.1. SCHEMATIC DIAGRAM FOR SINGLE-PHASE SIMULATION

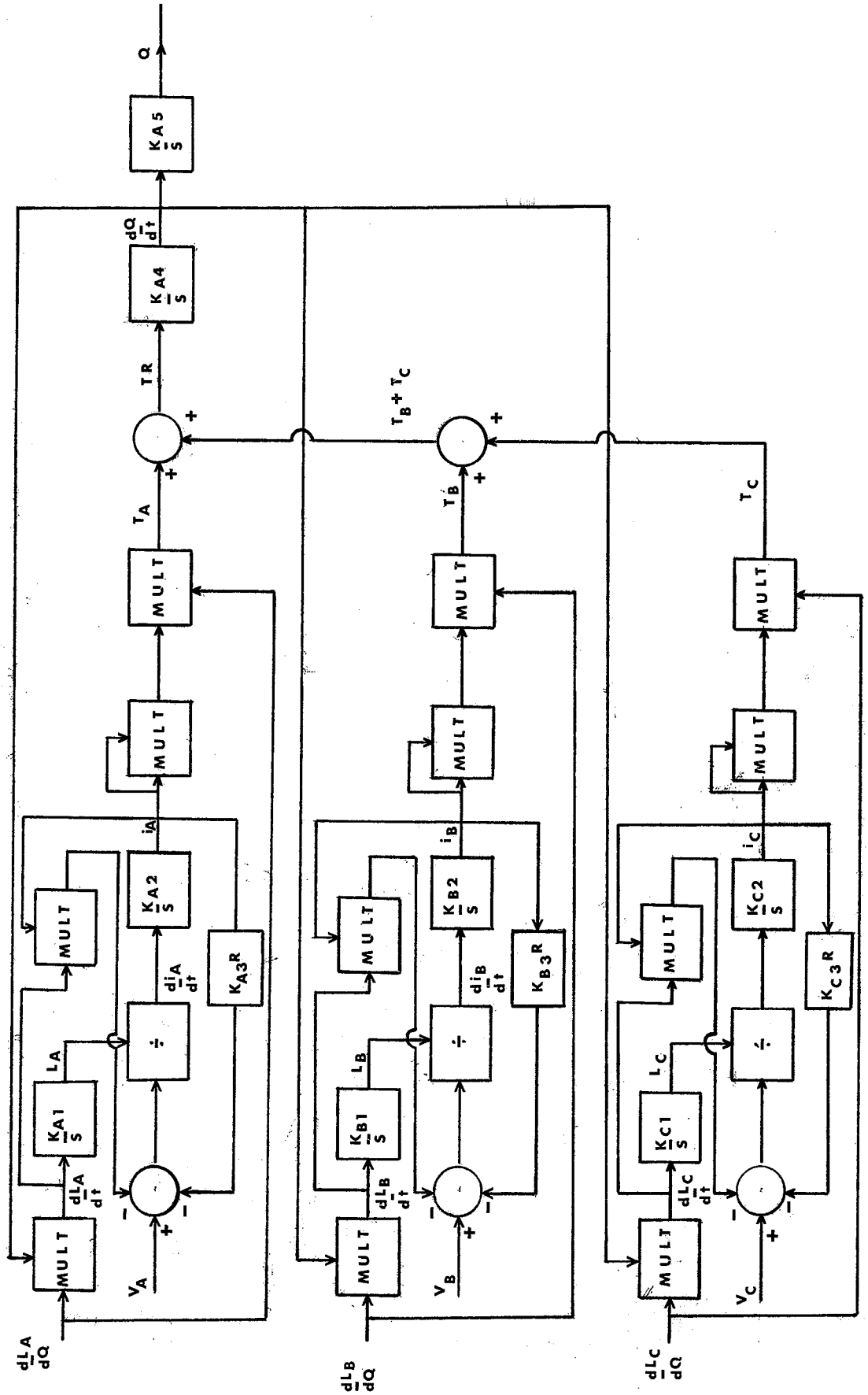

Fig.2.2.2. BLOCK DIAGRAM FOR A THREE-PHASE MACHINE

$$Jh^2 \frac{d^2\theta}{dT^2} + K_1 h \frac{d\theta}{dT} + T_L = TR = \frac{1}{2} i^2 \frac{dL}{d\theta} \quad \ldots\ldots\ldots 2.2.3.$$

$$\text{and} \quad V = iR + Lh \frac{di}{dT} + ih \frac{dL}{dT} \quad \ldots\ldots\ldots 2.2.4.$$

MAGNITUDE SCALING:

In the following equations, subscripted K's represent the magnitude scale factors for respective variables. Cm is the maximum computer voltage, i.e., 10 volts.

$$K_\theta = \frac{\max|\theta|}{cm} = \frac{3}{10} = 0.3 \text{ rad/V}$$

$$\therefore \theta = 0.3U \text{ radians}$$

$$K_{\frac{d\theta}{dT}} = \frac{\max|d\theta/dT|}{cm} = \frac{6}{10} = 0.6 \text{ rad/s-V}$$

$$\frac{d\theta}{dT} = 0.6S \text{ rad/sec}$$

$$K_{\frac{d^2\theta}{dT^2}} = \frac{\max|d^2\theta/dT^2|}{cm} = \frac{10^3}{10} = 10^2 \text{ rad/s}^2\text{-V}$$

$$\therefore \frac{d^2\theta}{dT^2} = 10^2 G \text{ rad/s}^2$$

$$K_V = \frac{\max|V|}{cm} = \frac{20}{10} = 2 \text{ V/V}$$

$$\therefore V = 2A \text{ volts}$$

$$K_i = \frac{\max|i|}{cm} = \frac{20}{10} = 2 \text{ A/A}$$

$$\therefore i = 2B \text{ amps}$$

$$K_{\frac{dL}{dT}} = \frac{\max\left|\frac{dL}{d\theta}\right| \cdot \left|\frac{d\theta}{dT}\right|}{cm} = \frac{6 \times 10^{-3} \times 6}{10} = 0.36 \times 10^{-2} \text{ H/s-V}$$

$$\therefore \frac{dL}{dT} = 0.36 \times 10^{-2} M \text{ H/s}$$

$$K_L = \frac{\max|L|}{cm} = \frac{1.5 \times 10^{-2}}{10} = 1.5 \times 10^{-3} \text{ H/V}$$

$$\therefore \quad L = 1.5 \times 10^{-3} D \quad H$$

$$K_{\frac{di}{dT}} = \frac{2 \times 10^2}{10} = 20 \text{ A/s-V}$$

$$\therefore \quad \frac{di}{dT} = 20 \; E \quad A/s \qquad A/S$$

$$K_{\frac{dL}{d\theta}} = \frac{\max|dL/d\theta|}{cm} = \frac{6 \times 10^{-3}}{10} = 6 \times 10^{-4} \text{ H/rad-V}$$

$$\therefore \quad \frac{dL}{d\theta} = 6 \times 10^{-4} \; F \text{ H/rad}$$

U, S, G, A, B, M, D, E and F represent computer voltages for $\theta, \frac{d\theta}{dT}, \frac{d^2\theta}{dT^2}$, V, i, $\frac{dL}{dT}$, L, $\frac{di}{dT}$, and $\frac{dL}{d\theta}$ respectively.

From the above, we can write the following equations:

$$U = 0.2 \times 10 \int S \, dT + U(o), \qquad \ldots\ldots\ldots 2.2.5.$$

$$S = \int (0.2 \, B^2 F - 0.9996 \times 10^4 \, SK_1 - 0.1666 \times 10^3 \, T_L) \, dT \qquad \ldots\ldots\ldots 2.2.6.$$

$$E = \frac{1}{D} [0.6666A - 0.3333 \times 10 \, B - 0.24 \, BM] \qquad \ldots\ldots\ldots 2.2.7.$$

$$B = 10 \int E \, dT + B(o) \qquad \ldots\ldots\ldots 2.2.8.$$

$$D = 0.24 \times 10 \int M \, dt + D(o) \qquad \ldots\ldots\ldots 2.2.9.$$

$$\frac{dL}{d\theta} = \frac{dL}{dT} / / \frac{d\theta}{dT} = 6 \times 10^{-3} \frac{M}{S} = 6 \times 10^{-4} F$$

$$\therefore \frac{M}{S} = 0.1 \; F$$

Equations 2.2.5., 2.2.6., 2.2.7., 2.2.8., and 2.2.9. are simulated as usual on an Analog computer. Since $\frac{dL}{d\theta}(\theta)$ changes its sign every ninety degrees, the second harmonic of $\sin\theta$ is generated as shown, (marked as II) in Fig. 2.2.1. and accomplish the objective of generating $\frac{dL}{dQ}$ (Q) using a comparator.

The parameters chosen for this example are given in Appendix 2.

The analog model refers to the rectangular voltage pulses and triangular inductance waveforms.

The schematic and block diagrams given in Figs. 2.2.1. and 2.2.2.

are considerably different from the ones published by Kuo, Singh and Yackel[2]. It appears that they have assumed inductances constant. Since no simulation results have been shown, those block diagrams[2] are probably only of theoretical importance.

A discussion of the results is taken up in Chapter 4.

2.3 General analysis of a variable-reluctance stepping motor

The motor considered here is similar to the one described in section 2.1. except that it consists of P number of units for P phases in place of three units for three phases. The rotors of all units are aligned axially and each unit is staggered by 360/TXP degrees on the stator. A three phase ten tooth machine is shown in Fig. 2.3.1.

The units may be excited, one at a time or in other possible combinations to achieve step angles smaller than the one, when only one coil is excited at a time.

The inductance and voltage waveforms are shown in Figs. 2.3.2. and 2.3.3. respectively. The inductance waveforms are periodic functions of θ (mechanical angle) with a period of 2α, where,

$$\alpha = \frac{P}{2} \cdot \theta_s \qquad \ldots\ldots\ldots \quad 2.3.1.$$

and $$\theta_s = \frac{360}{P \cdot T}$$

The number of teeth on the stator unit are equal to the number of rotor teeth for the type of motors analyzed in this thesis.

The voltage waveforms are periodic. If K is the number of pulses per second, $W = \frac{1}{K}$ and since there are P phases, the period of the voltage waveforms is PW, when only one unit is excited at a time.

The inductance and voltage waveforms described above are represented by Fourier Series according to Appendix I. Therefore, we have

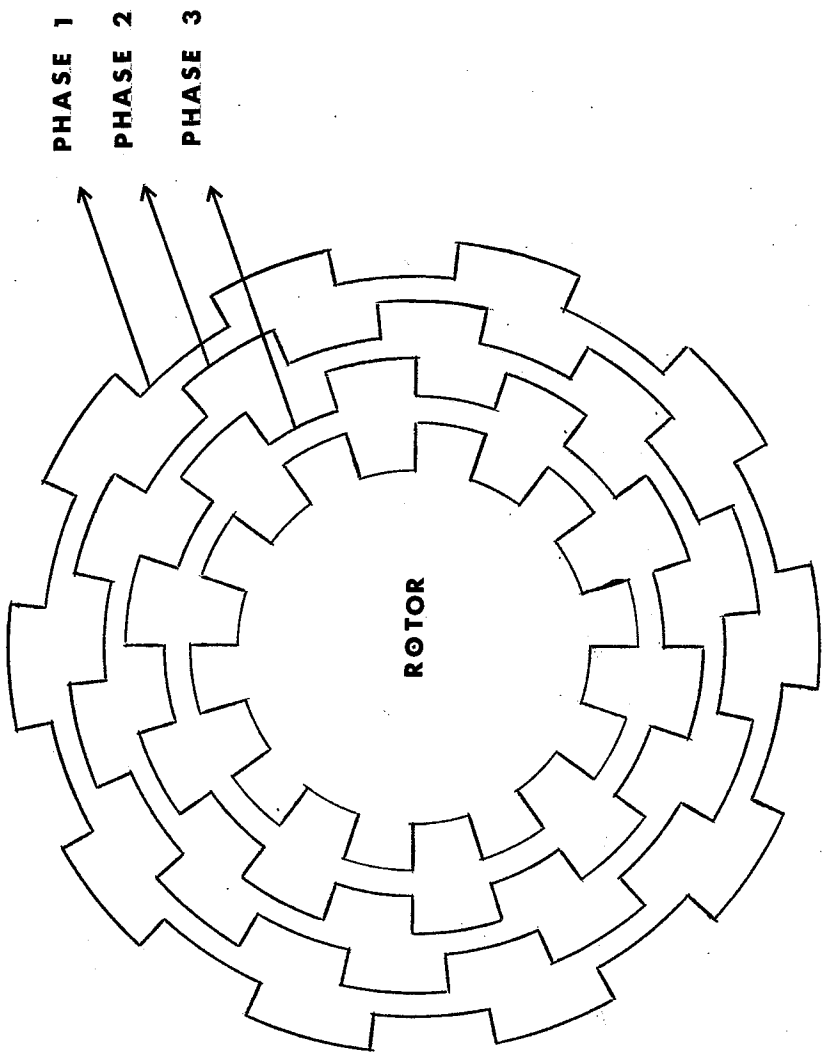

Fig.2.3.1. THREE-PHASE TEN-TOOTH MACHINE

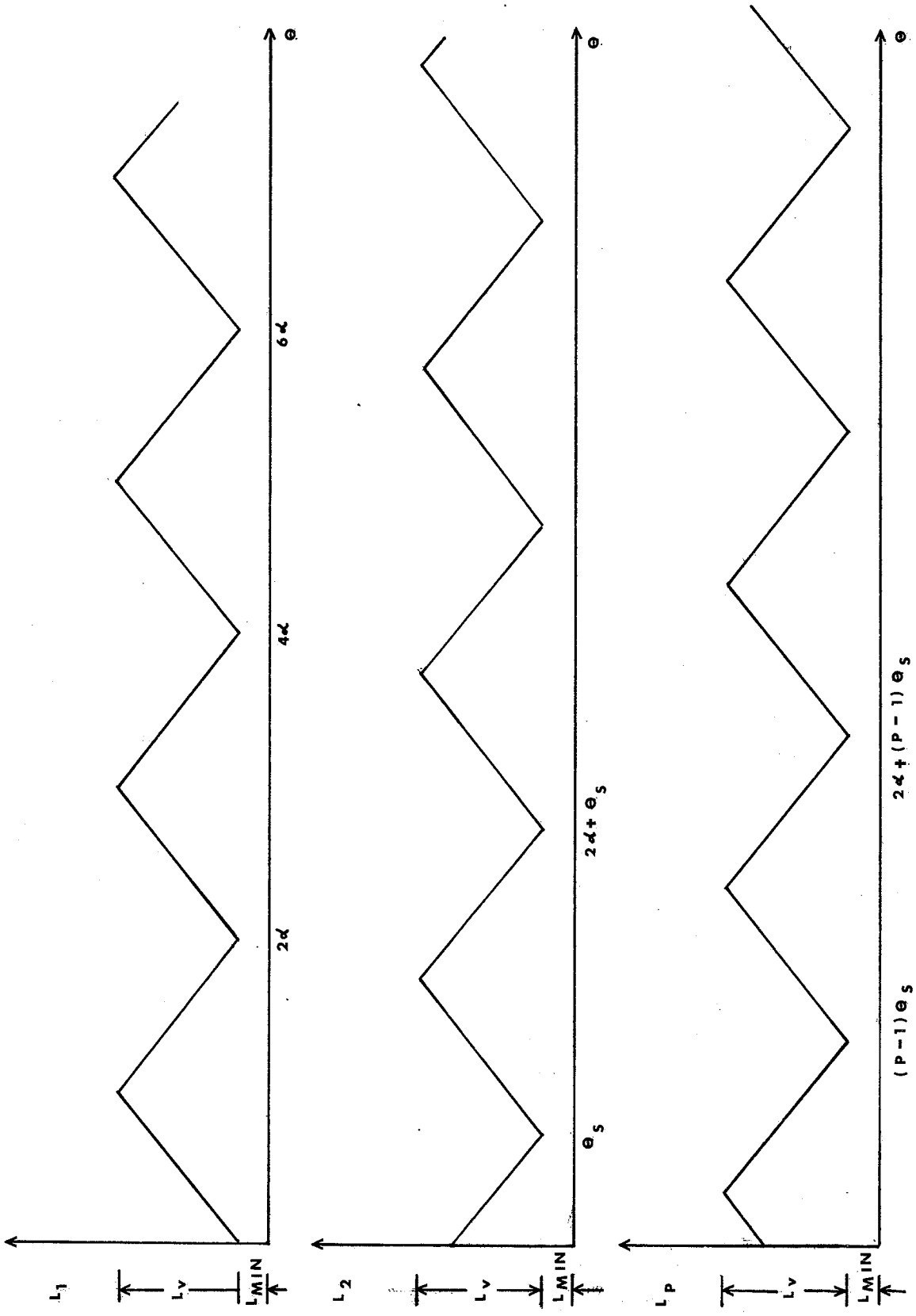

Fig.2.3.2. INDUCTANCE WAVEFORMS FOR A MULTI-STACK MACHINE

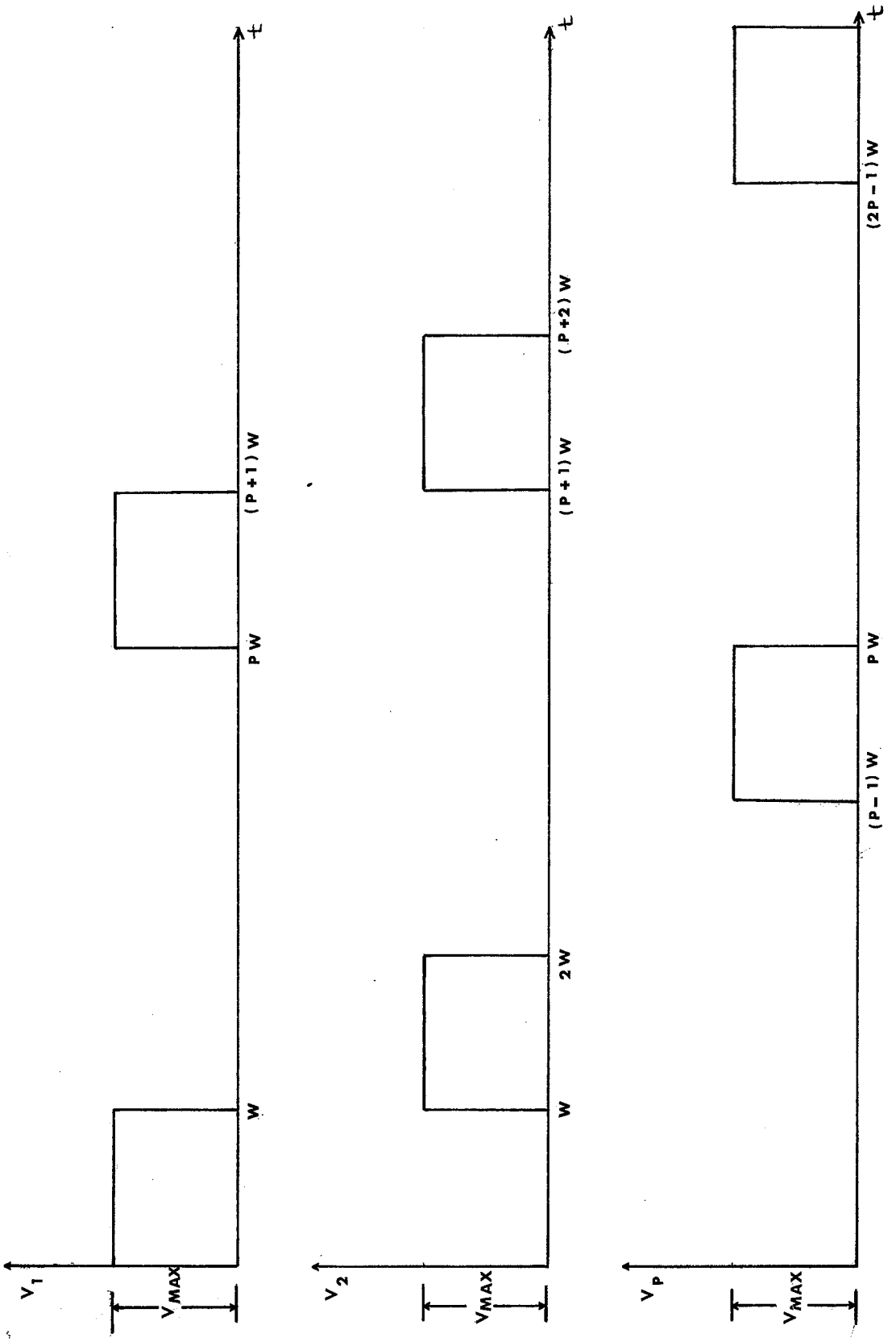

Fig.2.3.3. VOLTAGE WAVEFORMS FOR A MULTI-STACK MACHINE

$$L_1(\theta) = \frac{L_v}{2} + \frac{2L_v}{\pi^2} \sum_{n=1}^{\infty} \frac{1}{n^2} \{(-1)^n - 1\} \cos \{\frac{n\pi}{\alpha}(\theta)\} + L_{min}$$

..... 2.3.3.

$$L_2(\theta) = \frac{L_v}{2} + \frac{2L_v}{\pi^2} \sum_{n=1}^{\infty} \frac{1}{n^2} \{(-1)^n - 1\} \cos \{\frac{n\pi}{\alpha}(\theta-\theta_s)\} + L_{min}$$

..... 2.3.4.

and $$L_p(\theta) = \frac{L_v}{2} + \frac{2L_v}{\pi^2} \sum_{n=1}^{\infty} \frac{1}{n^2} \{(-1)^n - 1\} \cos \{\frac{n\pi}{\alpha}(\theta-(P-1)\theta_s)\} + L_{min}$$

..... 2.3.5.

Also,

$$V_1(t) = \frac{V_{max}}{P} + \sum_{n=1}^{\infty} \left[\frac{V_{max}}{n\pi} \{\sin(\frac{2n\pi}{P}) \cos(\frac{2n\pi t}{Pw}) + (1 - \cos\frac{(2n\pi)}{P}) \sin(\frac{2n\pi t}{Pw})\}\right]$$

..... 2.3.6.

$$V_2(t) = \frac{V_{max}}{P} + \sum_{n=1}^{\infty} \left[\frac{V_{max}}{n\pi} \{\sin(\frac{2n\pi}{P}) \cos(\frac{2n\pi(t-w)}{P}) + (1 - \cos\frac{(2n\pi)}{P}) \sin(\frac{2n\pi(t-w)}{Pw})\}\right]$$

..... 2.3.7.

and $$V_p(t) = \frac{V_{max}}{P} + \sum_{n=1}^{\infty} \left[\frac{V_{max}}{n\pi} \{\sin(\frac{2n\pi}{P}) \cos(\frac{2n\pi(t-(P-1)w)}{Pw}) + (1 - \cos(\frac{2n\pi}{P})) \sin(\frac{2n\pi(t-(P-1)w)}{Pw})\}\right]$$

..... 2.3.8.

The current in any one of the stator coils, when excited by voltage is given by

$$i = \frac{V}{R + \frac{dL}{d\theta} \cdot \frac{d\theta}{dt}} \left[1 - e^{-(R + \frac{dL}{d\theta} \cdot \frac{d\theta}{dt})\, t/L}\right] \quad \ldots 2.3.9.$$

as derived in section 2.1.

Torques produced by all phases can be added algebraically to give the resultant torque. Therefore,

$$TR = \frac{1}{2}(i_1)^2 \frac{dL_1(\theta)}{d\theta} + \frac{1}{2}(i_2)^2 \frac{dL_2(\theta)}{d\theta} + \ldots\ldots + \frac{1}{2}(i_p)^2 \frac{dL_p(\theta)}{d\theta} \quad \ldots\ldots 2.3.10$$

$\frac{dL_1(\theta)}{d\theta}$, $\frac{dL_2(\theta)}{d\theta}$, ... $\frac{dL_p(\theta)}{d\theta}$ are obtained

directly from equations 2.3.3., 2.3.4., and 2.3.5., by differentiating w.r.t.θ. Therefore,

$$\frac{dL_1(\theta)}{d\theta} = \frac{2L_v}{\pi\alpha} \sum_{n=1}^{\infty} \frac{1}{n} \{1 - (-1)^n\} \sin \frac{n\pi\theta}{\alpha} \quad \ldots\ldots\ldots 2.3.11.$$

$$\frac{dL_2(\theta)}{d\theta} = \frac{2L_v}{\pi\alpha} \sum_{n=1}^{\infty} \frac{1}{n} \{1-(-1)^n\} \sin \frac{n\pi(\theta-\theta_s)}{\alpha} \quad \ldots\ldots\ldots 2.3.12.$$

and $$\frac{dL_p(\theta)}{d\theta} = \frac{2L_v}{\pi\alpha} \sum_{n=1}^{\infty} \frac{1}{n} \{1 - (-1)^n\} \sin \left(\frac{n\pi(\theta-(p-1)\theta_s}{\alpha}\right). \quad 2.3.13.$$

Instantaneous values of speed and position, i.e., $\frac{d\theta(t)}{dt}$ and $\theta(t)$ are obtained by using the equation

$$TR = J \frac{d^2\theta}{dt^2} + K_1 \frac{d\theta}{dt} + K_2\theta + T_L \quad \ldots\ldots 2.3.14$$

Values of $i_1(t)$, $i_2(t)$, ... $i_p(t)$ are obtained by substituting respective instantaneous values of $\frac{dL(\theta)'s}{d\theta}$, $\frac{d\theta(t)'s}{dt}$, $L(\theta)$'s and $V(t)$'s in equation 2.3.9. Torque is obtained using equation 2.3.10.

Hence the performance characteristics are predicted for a particular motor, by proper substitution of the number of teeth and phases of the motor together with its electrical and mechanical parameters. The computer programs are capable of simulating multi-tooth and multi-phase machines. It is necessary because there is a growing trend to go in for more than three phase machines.

The simulation results are discussed in Chapter 4.

CHAPTER 3

ABSOLUTE AND SATISFACTORY PERFORMANCE LIMITS

Stepping motors are generally used for single step operation or multi-step operation, under various load conditions. The need for simple algebraic relations for predicting the satisfactory performance limits under different modes of operation is thus not only appreciable but desirable, because of the present interest in the standardization of conventions and parameters which define the performance of the stepping motors.

For this very purpose, a few terms are defined below. They are expressed as algebraic functions of the electrical and mechanical parameters of the motor and the load conditions later in this chapter to eliminate the necessity of computer simulation and a step-by-step calculation which would otherwise be necessary.

(a) Maximum "Pull-in" Pulse Rate: - is the maximum pulse rate at which the motor will respond to in either direction from the rest position without missing a step. There are two distinct values, for a particular load condition, one for a single step operation and second for multiple step operation. These are defined as maximum "Pull-in" frequency, as applicable to single step operation and simply maximum "Pull-in" frequency, respectively.

(b) Maximum "Pull-out" pulse rate: - is defined as the maximum frequency at which the motor will operate satisfactorily without loss of synchronizm, after having started the motor at or less than maximum pull-in frequency. Motors exhibit considerable amount of instability if started at pull-out frequency. This is also known as the maximum operating frequency.

In the following, algebraic equations have been derived and verified for the limiting pull-in and pull-out operation of VR stepping motors. Such expressions have not been available in the published literature to the best of the knowledge of the author. These expressions result in a direct calculation which would otherwise be obtained from a number of trials using step-by-step calculations on a digital computer.

3.1.1 Pull-in frequency - for single step operation

The dynamic equation of the system is

$$J\frac{d^2\theta}{dt^2} + K_1\frac{d\theta}{dt} + K_2\theta + T_L = \frac{1}{2}i^2\frac{dL}{d\theta} \qquad \ldots\ldots\ldots 3.1.1.$$

The third term of equation 3.2.1. is usually negligibly small and is neglected here. Therefore,

$$J\frac{d^2\theta}{dt^2} + K_1\frac{d\theta}{dt} + T_L = \frac{1}{2}i^2\frac{dL}{d\theta} \qquad \ldots\ldots\ldots 3.1.2.$$

The voltage equation for any coil is given by

$$V(t) = i(t)R + L(\theta)\frac{di(t)}{dt} + i(t)\frac{dL(\theta)}{d\theta}\frac{d\theta(t)}{dt} \qquad \ldots\ldots\ldots 3.1.3.$$

Solution for $i(t)$ cannot be obtained directly from equation 3.1.3., as it stands. However, using step-by-step integration, the simulation results for current showed that this curve can be fitted very closely, from no load to approximately half the full load torque, by

$$i = K(1 - e^{-t/T_a}) \qquad \ldots\ldots\ldots 3.1.4.$$

as shown in Fig. 3.1.1. where $K = V/R$ and T_a is the average time constant of the winding. (The average of L being taken between the stable starting value of L and maximum value of L).

Substituting the value of i from equation 3.1.4. into equation 3.1.2., we get

$$J\frac{d^2\theta}{dt^2} + K_1\frac{d\theta}{dt} + T_L = \frac{1}{2}K^2(1 - e^{-t/T_a})^2\frac{dL}{d\theta}$$

or

$$J\frac{d^2\theta}{dt^2} + K_1\frac{d\theta}{dt} + T_L = A(1 - e^{-t/T_a})^2$$

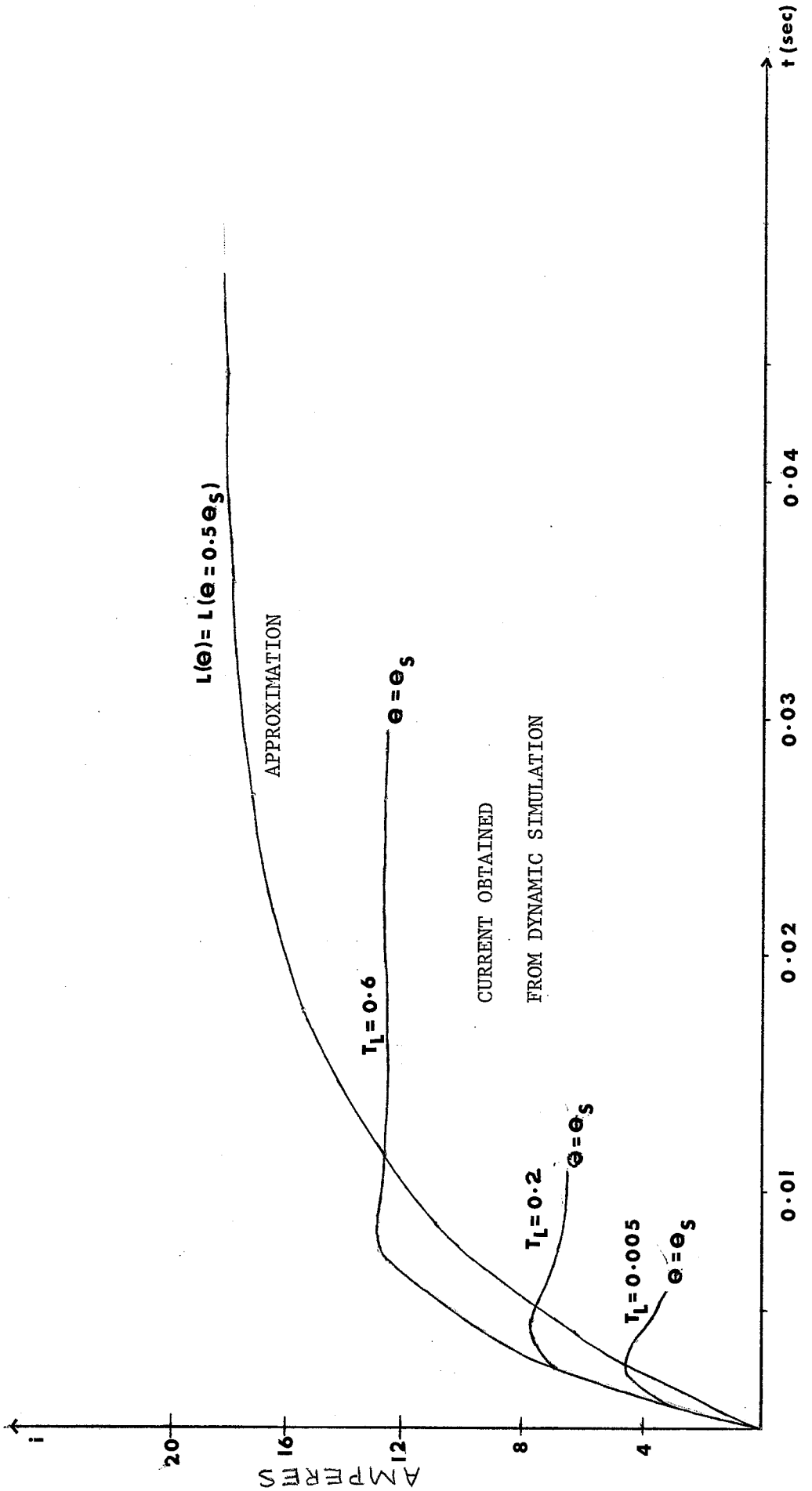

Fig.3.1.1. APPROXIMATED AND ACTUAL CURRENTS

where $A = \frac{1}{2} K^2 \frac{dL}{d\theta}$ = a constant, for a triangular inductance waveform

$$\text{or} \quad \frac{d^2\theta}{dt^2} + \frac{K_1}{J} \frac{d\theta}{dt} + \frac{T_L}{J} = \frac{A}{J} (1 - e^{-t/T_a})^2$$

$$\text{or} \quad \frac{d^2\theta}{dt^2} + a \frac{d\theta}{dt} = b(1 - e^{-t/T_a})^2 - c \qquad \ldots\ldots\ldots 3.1.5.$$

where $a = \frac{K_1}{J}$, $b = \frac{A}{J}$ and $c = \frac{T_L}{J}$

The motor does not move until the motor torque equals the load torque. Let t_1 be the time when motor torque becomes equal to load torque. This can be obtained by equating

$$T_L = A(1 - e^{-t_1/T_a})^2 \qquad \ldots\ldots\ldots 3.1.6.$$

$$\text{or} \qquad t_1 = T_a \log_e \left[\frac{1}{1 - (T_L/A)^{1/2}}\right] \qquad \ldots\ldots\ldots 3.1.7.$$

Therefore, the equation for dynamics of the motor such that $\theta = 0$ at $t = 0$ and motor torque always greater than load torque for $t \geq 0$ will be

$$\frac{d^2\theta}{dt^2} + a \frac{d\theta}{dt} = b \left[1 - e^{-(t + t_1)/T_a}\right]^2 - c \qquad \ldots\ldots\ldots 3.1.8.$$

Let $\frac{d\theta}{dt} = x_1$ and substitute in equation 3.1.8. Therefore,

$$\frac{dx_1}{dt} + a x_1 = b[1 - e^{-(t + t_1)/T_a}]^2 - c$$

The general solution of this equation is

$$x_1 = c_1 e^{-at} + \frac{(b - c)}{a} - \frac{2 b T_a}{(a T_a - 1)} e^{-t_1/T_a} e^{-t/T_a} + \frac{b T_a}{(a T_a - 2)} e^{-2t_1/T_a} e^{-2t/T_a}$$

Therefore,

$$\frac{d\theta}{dt} = c_1 e^{-at} + \frac{(b - c)}{a} - \frac{2 b T_a}{(a T_a - 1)} e^{-t_1/T_a} e^{-t/T_a}$$

$$+ \frac{b T_a}{(a T_a - 2)} e^{-2t_1/T_a} e^{-2t/T_a} \qquad \ldots\ldots\ldots 3.1.9.$$

For maximum pull-in frequency, at

$$t = 0, \quad \frac{d\theta}{dt} = 0$$

This condition is easily justified for pull-in frequency since the motor has to start from zero initial velocity. But condition will certainly be different if one is looking for the maximum operating frequency range for variation in load, because motor is likely to have some initial speed when the next pulse is applied. Incorporating the initial condition in equation 3.1.8. and substituting the value of c_1 back in there, we get

$$\frac{d\theta}{dt} = \left[\frac{2 b T_a}{(a T_a - 1)} e^{-t_1/T_a} - \frac{b T_a}{(a T_a - 2)} e^{-2t_1/T_a} - \frac{(b - c)}{a}\right]$$

$$e^{-at} + \frac{(b - c)}{a} - \frac{2 b T_a}{(a T_a - 1)} e^{-t_1/T_a} e^{-t/T_a}$$

$$+ \frac{b T_a}{(a T_a - 2)} e^{-2t_1/T_a} e^{-2t/T_a}$$

Let $X = \frac{2 b T_a}{(a T_a - 1)} e^{-t_1/T_a}$, $Y = \frac{b T_a}{(a T_a - 2)} e^{-2t_1/T_a}$

and $Z = \frac{(b - c)}{a}$

$$\therefore \frac{d\theta}{dt} = (X - Y - Z) e^{-at} + Z - X e^{-t/T_a} + Y e^{-2t/T_a}$$

Integrating w.r.t.t, we get

$$\theta = (X - Y - Z) \frac{e^{-at}}{-a} + Zt - \frac{X e^{-t/T_a}}{-1/T_a} + Y \frac{e^{-2t/T_a}}{-2/T_a} + c_2 \qquad \ldots\ldots 3.1.10.$$

At $t = 0$, $\theta = 0$, assuming that the motor is started from a stable position. Using the initial condition for finding C_2 and substituting back in equation 3.1.10., we get

$$\theta = \left(\frac{X - Y - Z}{a}\right)(1 - e^{-at}) - X\,T_a(1 - e^{-t/T_a}) + \frac{Y\,T_a}{2}(1 - e^{-2t/T_a}) + Z\,t$$

By expanding the exponential functions and neglecting fifth and higher order of t and simplifying, we get

$$\theta = \frac{(X - Y)a}{2}\left[\frac{a\,t^3}{3} - t^2 - \frac{a^2t^4}{12}\right] - \left(\frac{b - c}{2}\right)\left[\frac{a\,t^3}{3} - t^2 - \frac{a^2t^4}{12}\right] + \frac{X}{2\,T_a}\left[t^2 - \frac{t^3}{3\,T_a} + \frac{t^4}{12\,T_a^2}\right] + \frac{Y}{T_a}\left[\frac{2\,t^3}{3\,T_a} - t^2 - \frac{t^4}{3\,T_a^2}\right]$$

Neglecting damping coefficient K_1, $a = \frac{K_1}{J}$ becomes zero

$$\therefore\ \theta = \frac{X}{2\,T_a}\left[t^2 - \frac{t^3}{3\,T_a} + \frac{t^4}{12\,T_a^2}\right] + \frac{Y}{T_a}\left[\frac{2\,t^3}{3\,T_a} - t^2 - \frac{t^4}{3\,T_a^2}\right] + \frac{b\,t^2}{2} - \frac{c\,t^2}{2}$$

or $$\theta = A_1t^4 + A_2t^3 + A_3t^2 \qquad \ldots\ldots\ldots \text{3.1.11.}$$

where $A_1 = \frac{X}{24\,T_a^3} + \frac{Y}{3\,T_a^3}$, $A_2 = \frac{2Y}{3\,T_a^2} - \frac{X}{6\,T_a^2}$

and $A_3 = \frac{b}{2} - \frac{C}{2} + \frac{X}{2\,T_a} - \frac{Y}{T_a}$

If load torque is simply an inertial load, i.e., $T_L = 0$, t_1 becomes zero and equation 3.1.11 reduces simply to

$$\theta = \frac{b\, t^4}{12\, T_a^2}$$

Allowing no overshot, which is an undesirable feature in precision control and motor moving the exact step angle, θ_s, during the pulse duration, we have the condition for the maximum pull-in frequency

$$\text{at} \qquad t = \omega_{ss}, \quad \theta = \theta_s$$

$$\therefore \quad \omega_{ss} = \left[\frac{12\theta_s\, T_a^2}{b}\right]^{1/4} \qquad T_L = 0 \;, \quad K_1 = 0$$

If $T_L \neq 0$, value of ω_{ss1} can be obtained by solving the polynomial given in equation 3.1.11 and selecting the minimum real root. Here,

$$\omega_{ss} = \omega_{ss1} + t_1$$

$\therefore$ FIN SS = maximum pull-in frequency for single step operation =

$1/\omega_{ss}$ ..... 3.1.12.

The curves depicting the effect of load torque on maximum pull-in frequency for single step operation, from computer simulation and the expression 3.1.12, are given in Figure 3.1.2.

The results are reasonably good while the load torque is less than half of the maximum torque motor can produce. It should also be noted from Fig. 3.1.2. that the load torque Vs. maximum pull-in frequency curve, as applied to single step positional control, from the computer simulation is always below the one obtained from expression 3.1.12. This is because of the fact that the motor will stay stationary until motor torque becomes equal to load torque and hence the voltage impressed on any of the stator coils will face less value of inductance than the one assumed in expression 3.1.4., until motor executes half of the step angle. This will cause comparatively sharper rise in current as compared to the initial assumption. However, after half of the step has been executed, excitation voltage faces higher value of inductance and current rise becomes less and less sharp. Also because of the term $i \frac{dL}{d\theta} \cdot \frac{d\theta}{dt}$ in the voltage equation, current will never reach the maximum value assumed, if the pulse is switched off immediately after the motor has executed the step angle as shown in Fig. 3.1.1. This easily indicates that if the value of the inductance is chosen such that this value occurs at θ_s, the predicted waveform will be better fitted to the actual one. However, in this case the two curves will cut at one

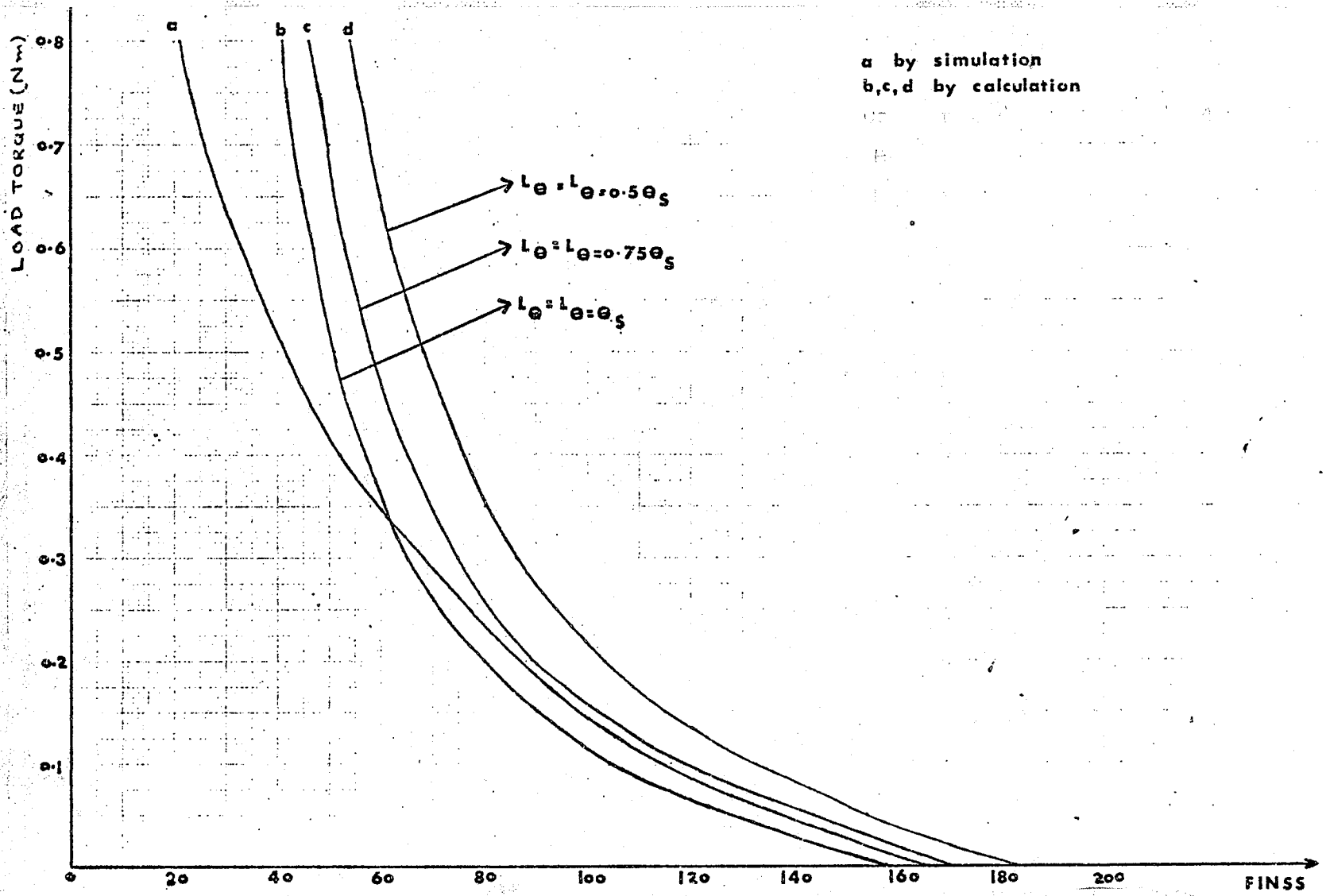

Fig.3.1.2. LOAD TORQUE/ FINSS CHARACTERISTICS

Frequency (P.P.S.)

point. So at low values of the load torque, the predicted frequency will be less than the one from computer simulation and for high value of torques vice versa, as shown in Fig. 3.1.2.

The shape of the curves match with the one published by Bell, Lowth and Shelley[6].

3.1.2 (b) Pull-in frequency for multiple step operation

From equation 3.1.11, we have

$$\theta = A_1 t^4 + A_2 t^3 + A_3 t^2 \qquad \ldots\ldots\ldots 3.1.12.$$

From the Fig. 3.1.3., it is easily seen that even if the motor does not execute the complete step angle during the first pulse, it may still synchronize with the next pulse provided that the motor has moved through the angle Ψ.

$$\alpha = \frac{P}{2} \cdot \theta_s$$

$$\theta_s = \frac{360}{P \cdot T}$$

$$\therefore \quad \phi = \alpha - \theta_s$$

$$= \frac{180}{T}\left[1 - \frac{2}{P}\right] = \frac{180}{T}\left[\frac{P-2}{P}\right]$$

$$\Psi = \theta_s - \phi = \frac{360}{P\,T} - \frac{180}{T}\left[\frac{P-2}{P}\right]$$

$$= \frac{180}{P\,T}\left[2 - P + 2\right] = \frac{180}{P\,T}(4 - P)$$

Therefore, for cases where $\theta_s > \phi$, for the maximum pull-in frequency, we have the condition

$$t = w_{MS} \quad , \quad \theta = \Psi$$

substituting this in equation 3.1.10.

$$\Psi = A_1 w_{MS}^{\ 4} + A_2 w_{MS}^{\ 3} + A_3 w_{MS}^{\ 2}$$

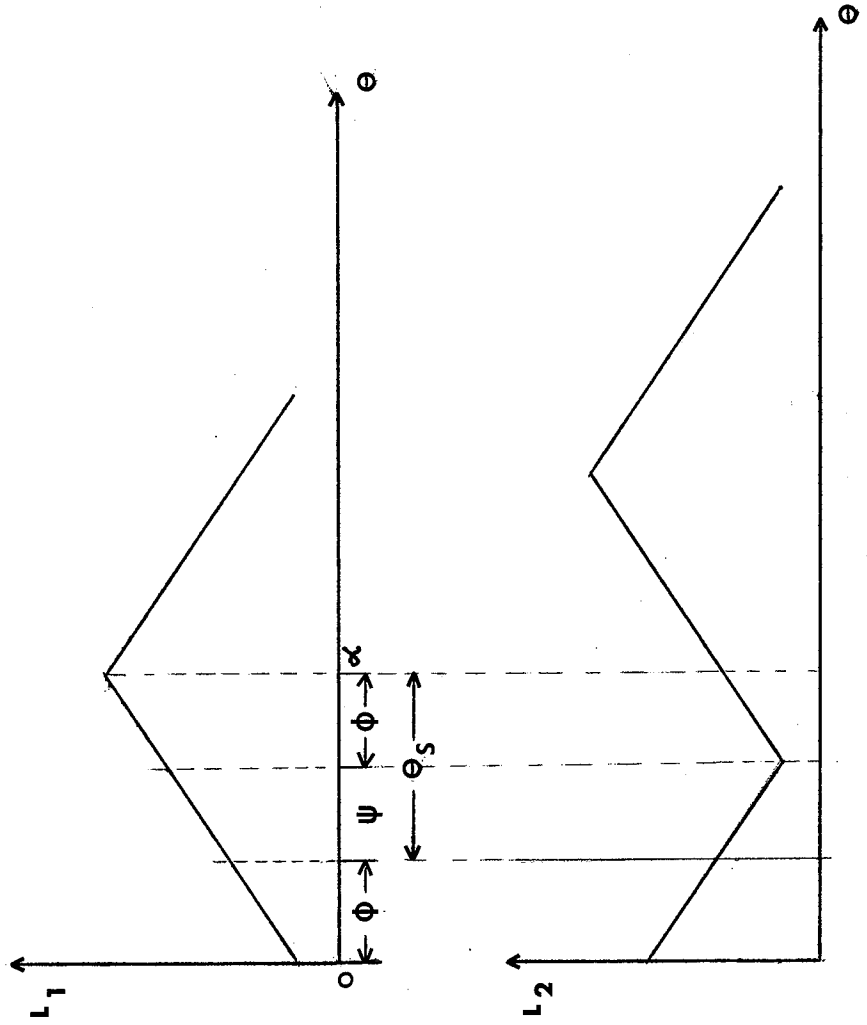

Fig.3.1.3. INDUCTANCES OF CONSECUTIVE PHASES

Therefore, w_{MS} can be obtained by slowing the above equation and selecting the minimum real root.

$\therefore$ FINMS = maximum pull-in frequency for multiple stepping

$$= 1/w_{MS} \qquad \ldots\ldots\ldots 3.1.13.$$

A comparison is shown in Fig. 3.1.4. between maximum pull-in frequency for single step operation and maximum pull-in frequency for multiple stepping.

For the reasons similar to given in section 3.1.(a), the value of the inductance to be chosen for calculations will be corresponding to the value of inductance at Ψ.

3.2. Pull-out or the maximum operating frequency

At the maximum operating frequency, after having started the motor at pull-in frequency, or just before the pull-out frequency, it can be reasonably assumed that

$$\frac{d\theta}{dt} = K_3 \qquad \ldots\ldots\ldots 3.2.1.$$

as shown in Fig. 3.2.1.

Where K_3 is the maximum value of speed, motor achieves, when started at maximum pull-in frequency allowing no overshoot. This can be obtained directly from equation 3.1.9,, by substituting w_{ss} for t.

$$\therefore K_3 = c_1 e^{-aw_{ss}} + \frac{(b-c)}{a} + \frac{b\,T_a}{(a\,T_a-2)} e^{-2w_{ss}/T_a} e^{-2t_1/T_a} - \frac{2b\,T_a}{(a\,T_a-1)} e^{-w_{ss}/T_a} e^{-t_1/T_a} \qquad \ldots\ldots\ldots 3.2.2.$$

Integrating equation 3.2.1., we get

$$\theta = K_3\, t$$

For maximum operating frequency,

$$\text{at} \quad t = w_{out} \quad , \quad \theta = \theta_s$$

$$\therefore \theta_s = K_3\, w_{out}$$

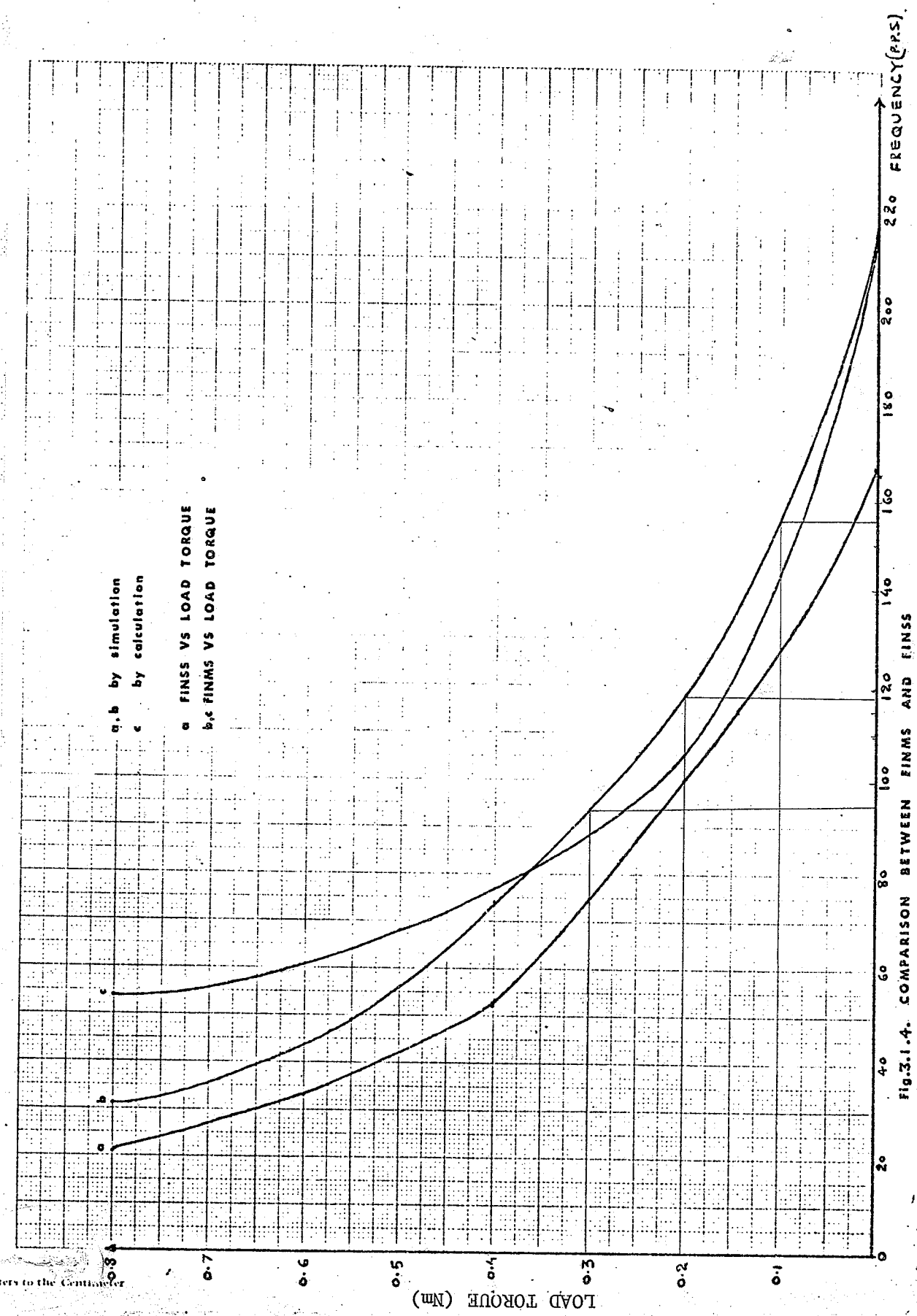

Fig.3.1.4. COMPARISON BETWEEN FINMS AND FINSS

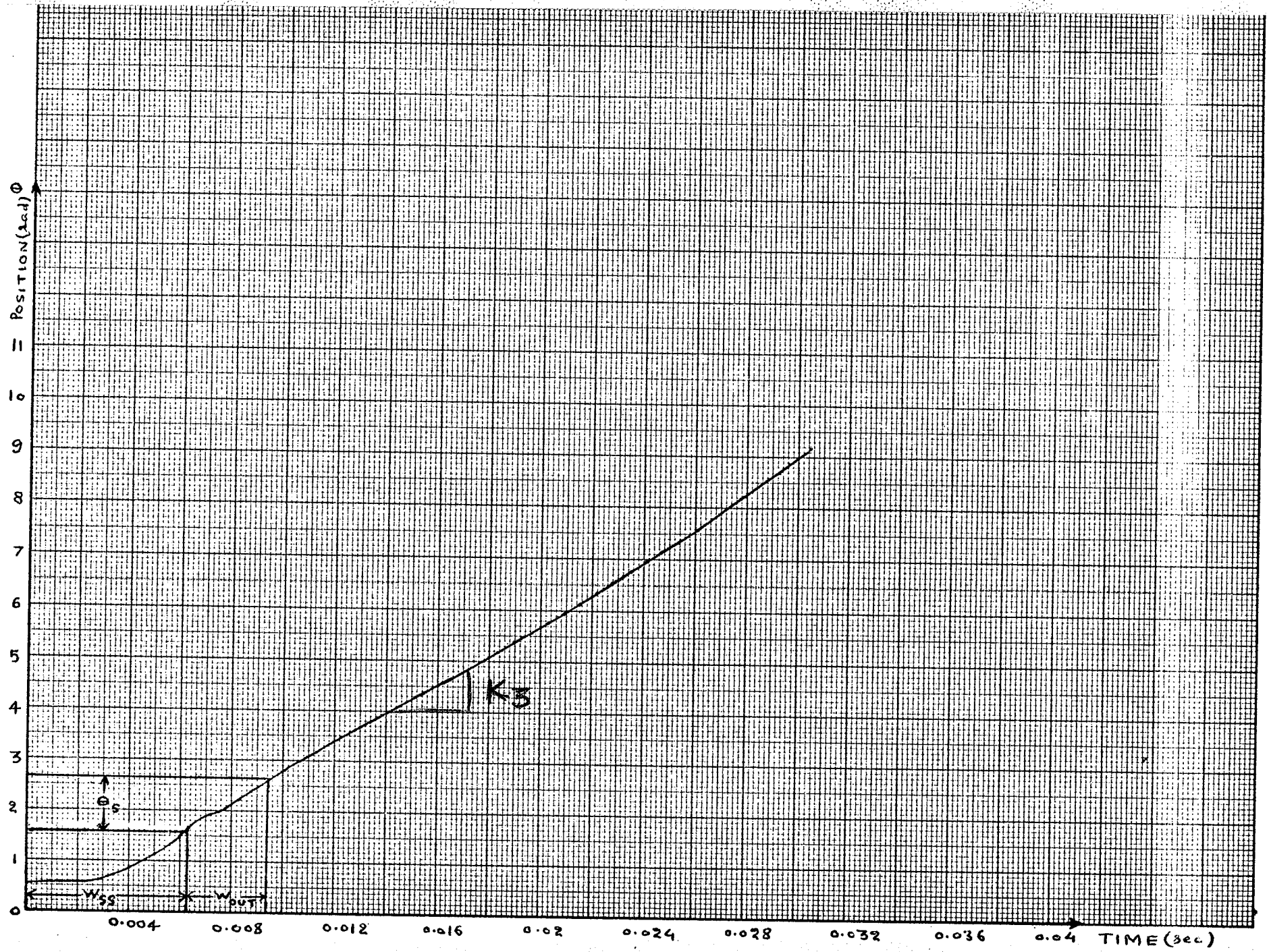

Fig. 3.2.1. POSITION/TIME CHARACTERISTICS

$$\text{or} \quad w_{out} = \frac{\theta_s}{K_3}$$

$$\therefore \quad \text{FOUT} = \text{Pull-out frequency} = \frac{1}{w_{out}} \qquad \ldots\ldots\ldots 3.2.3.$$

This is the maximum frequency at which the motor will operate without slippage. However, motor will execute considerable amount of instability if started at this value of frequency.

It should be noted that the damping effect is more predominant on the pull-out frequency as compared to the pull-in frequency.

3.3. Expression for the critical number of pulses

The expression for the current in any one of the stator coils, as derived in section 2.1., is

$$i = \frac{V}{R + \frac{dL}{d\theta} \cdot \frac{d\theta}{dt}} \left[1 - e^{-(R + \frac{dL}{d\theta} \cdot \frac{d\theta}{dt}) \frac{t}{L}} \right]$$

$$\text{or} \quad e^{-(R + \frac{dL}{d\theta} \cdot \frac{d\theta}{dt}) \frac{t}{L}} = 1 - \frac{i(R + \frac{dL}{d\theta} \frac{d\theta}{dt})}{V}$$

The variable, time (t), can be replaced by N x W, Where, N is the number of pulses elapsed at any time and W is the width of each pulse. Therefore,

$$e^{-(R + \frac{dL}{d\theta} \cdot \frac{d\theta}{dt}) \frac{Nw}{L}} = 1 - \frac{i(R + \frac{dL}{d\theta} \frac{d\theta}{dt})}{V} \qquad \ldots\ldots\ldots 3.3.1.$$

For synchronizm to be possible, w, the width of each pulse should at least be such that the rotor moves through a step angle. For this to be possible, the average speed, $\frac{d\theta}{dt}_{(a)}$, will have to be at least so much that the rotor moves through the step angle, θ_s, in w seconds. Therefore,

$$\frac{d\theta}{dt}_{(a)} = \frac{\theta_s}{w}$$

Replacing $\frac{d\theta}{dt}$ by $\frac{d\theta}{dt}_{(a)}$ and substituting $\frac{\theta_s}{w}$ for the latter in

equation 3.3.1., we get

$$e^{-(R + \frac{dL}{d\theta} \frac{\theta_s}{w}) \frac{Nw}{L}} = 1 - \frac{i(R + \frac{dL}{d\theta} \frac{\theta_s}{w})}{V} \quad \ldots\ldots\ldots 3.3.2.$$

If K is the number of pulses per second, $w = 1/K$, substituting for w in equation 3.3.2., we get

$$e^{-(R + \frac{dL}{d\theta} \cdot \theta_s \cdot K) \frac{N}{KL}} = 1 - \frac{i(R + \frac{dL}{d\theta} \cdot \theta_s \cdot K)}{V} \quad \ldots 3.3.3.$$

Since, we are considering only one pulse, we substitute $N = 1$ in equation 3.3.3. Therefore,

$$e^{-(R + \frac{dL}{d\theta} \cdot \theta_s \cdot K) \frac{1}{KL}} = 1 - \frac{i(R + \frac{dL}{d\theta} \cdot \theta_s \cdot K)}{V}$$

$\ldots\ldots\ldots 3.3.4.$

For the machine, having equal number of teeth in one stator unit and rotor,

$$\theta_s = \frac{2\pi}{P \cdot T}$$

where P = number of phases

and T = number of teeth

Also, $\frac{dL}{d\theta}$ can be replaced by $\frac{L_v}{\alpha}$ = constant, assuming that the inductance waveform is triangular.

where L_v = variable part of the inductance

and $\alpha = \frac{\text{waveform}}{\frac{P \cdot \theta_s}{2}}$

Substituting the values of θ_s and $\frac{dL}{d\theta}$ in equation 3.3.4., we have

$$e^{-(R + \frac{L_v}{\alpha} \cdot \frac{2\pi}{P \times T} \cdot K) \frac{1}{KL}} = 1 - \frac{i(R + \frac{L_v}{\alpha} \cdot \frac{2\pi}{P \times T} \cdot K)}{V}$$

Let $\frac{L_v}{\alpha} \frac{2\pi}{P \times T} = H$ = a constant for a particular motor

$$\therefore \quad e^{-(R + HK) \frac{1}{KL}} = 1 - \frac{i(R + HK)}{V} \quad \ldots\ldots\ldots 3.3.5.$$

Approximating the L.H.S. of equation 3.1.5. by first two terms,

we get

$$1 - (R + HK)\frac{1}{KL} = 1 - \frac{i(R + HK)}{V}$$

$$\text{or} \quad \frac{1}{KL} = \frac{i}{V} \qquad \ldots\ldots\ldots 3.3.6.$$

Current in any stator coil may be given by $G \frac{V}{R}$, where G is a constant. $G < 1$

$$\therefore \quad \frac{1}{KL} = \frac{G}{R}$$

$$\text{or} \quad w = G\frac{L}{R} \qquad \ldots\ldots\ldots 3.3.7.$$

Some of the inferences, not so obvious from the equation 3.3.7., are summarized as follows:

(i) The relation, $w = G\frac{L}{R}$, derived above is obtained directly from the current equation and does not take into consideration the effect of rotor inertia, load torque or damping. Obviously, this gives us the absolute upper operating frequency limit. There is every probability that some slippage will be present, even when there is no load on the machine. The less the inertia, the better the relationship will hold under no load conditions. Usually good design of a variable reluctance step motor provides a minimum rotor inertia.

(ii) The motor will not synchronize if started at the absolute upper frequency limit, even if started from a stable starting point. The possibility of its synchronizing with the voltage pulses, after a few steps have been missed, is however there. But this in turn depends upon the inertia, damping and load torque. However, it is strongly recommended not to either start or operate the motor at this value of the frequency because of the slippage - an undesirable feature in any control.

(iii) Since according to equation 3.3.7., minimum width of each pulse is inversely proportional to the resistance of the winding, it may

lead to fairly deceptive conclusion that one should be able to improve the absolute upper operating frequency limit, to improve the average speed between the steps, by including an external resistance in series with the stator coils. The answer is yes, provided the resistance included is of resonable value. But one should keep in mind that this will decrease the steady state value of the current and hence the torque that can be derived from the motor, because the torque is directly proportional to the square of the current.

(iv) As the width of each pulse keeps decreasing and when it starts approaching the ratio of inductance/resistance, the current fails to reach its steady state value and hence the output torque decreases.

CHAPTER 4

PERFORMANCE CHARACTERISTICS OF THE STEPPING MOTOR

Stepping motor operation can primarily be either single step or multi-step. Based on the simulation results, both analog and digital, developed in Chater 2. both of these modes of operation are discussed as follows:

4.1 Single step operation

Fig. 4.1.1. - 4.1.5. depict the performance characteristics of a simple three phase, two pole variable reluctance stepping motor.

Fig. 4.1.1. shows the effect of damping on the position/time response. It is easily noticed that damping is important for the design purposes, because this factor basically determines the overshoot, rise time and settling time. For all practical applications, system should be critically damped to obtain the optimum settling time. If the system is underdamped, it will execute considerable amount of oscillations before settling down which is an undesirable feature. Also, if the system is overdamped, though there are hardly any oscillations present, the settling time is increased. Hence, by choosing the critical value of damping, one is able to optimize the amount of oscillations before settling and also improve the settling time. For the particular motor chosen, the critical damping corresponds to $K_1 = 0.0003$. The parameters of this particular motor are given in Appendix 2.

It may be seen from the inductance waveforms for the above machine given in Fig. 2.1.2. that the stable point for operation of phase A is at 30° from the reference chosen. When phase A is excited, the rotor moves in such a way that there is a path of minimum reluctance for the

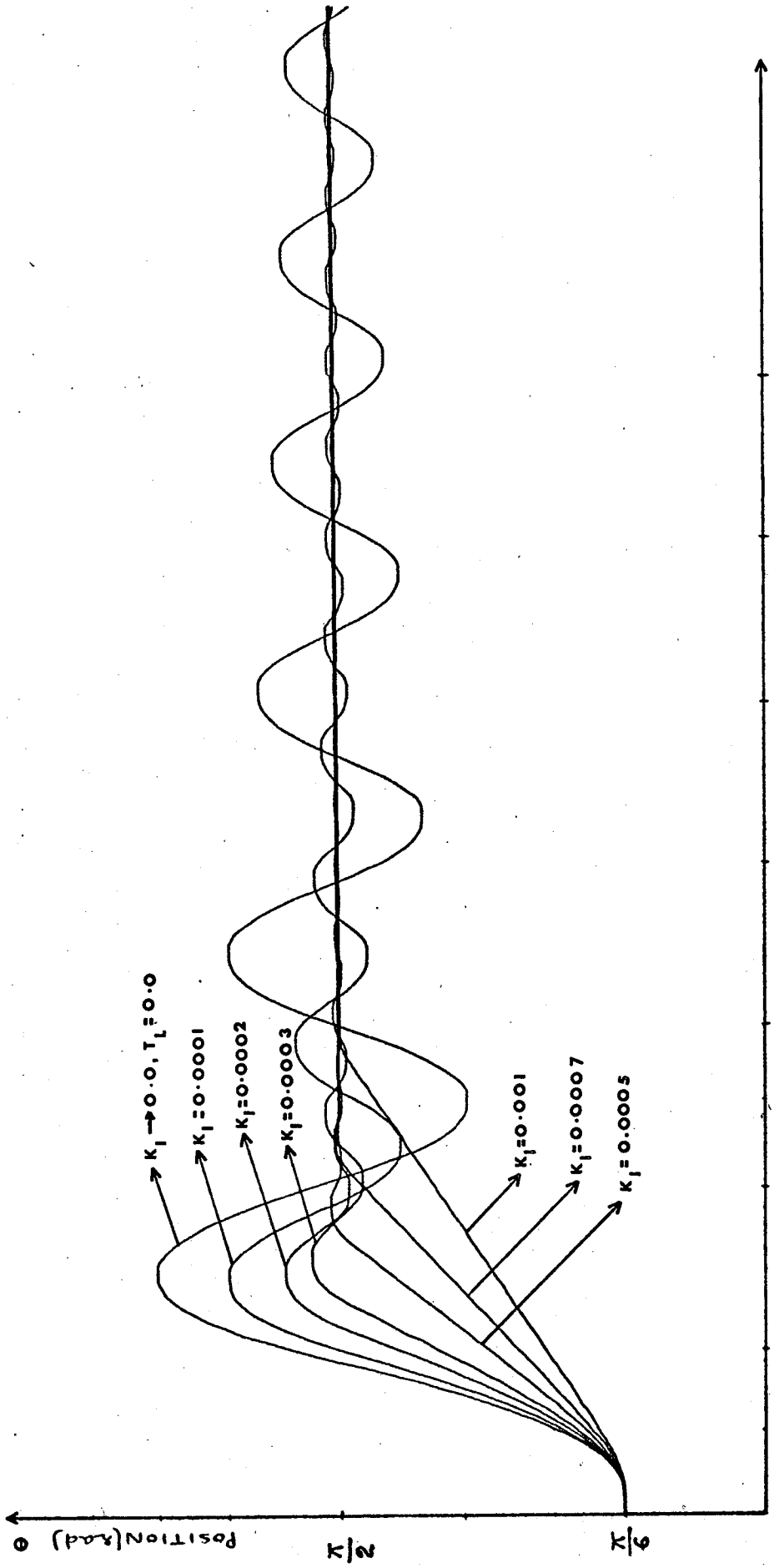

Fig.4.1.1. EFFECT OF DAMPING ON POSITION/TIME CHARACTERISTICS OF THE MOTOR

flux. The motor keeps turning and overshoots the stable starting point for phase B i.e., 90°, because of its initial velocity even when $\frac{dL}{d\theta}$ for phase A has become negative. However, negative $\frac{dL}{d\theta}$ causes breaking action and starts moving the rotor in the opposite direction. In an attempt to get the stable point it overshoots again in the negative direction and this process repeats till the oscillations die out. The time at which the oscillations will die out will depend upon the amount of damping.

Fig. 4.1.2. depicts the effect of load torque in the position/time characteristics for one arbitararily chosen value of damping. As is seen from the figure, the overshoot becomes less and less with increasing values of the load torque. This is because of the fact that the accelerating torque available decreases as the load torque increases and hence, motor is able to achieve less speed with increasing load torques. If the value of load torque is expected to be fairly close to the maximum steady state torque motor can produce, it might be a good idea to choose a value of damping less than the critical damping value. It is because the accelerating torque will be quite small and hence only a little overshoot. Hence, to have a low value of damping will be preferable to improve the settling time, for load torques close to full load motor torques.

Fig. 4.1.3. gives speed/position characteristics with three different starting positions. If the motor is started from a position before the stable starting point, the magnitude of speed is always higher than the one, if the motor had been started from a stable starting position and vice versa if the motor is started from some point after the stable starting point, for the same value of load torque and damping. This is because the current will have more time to rise and hence higher acceler-

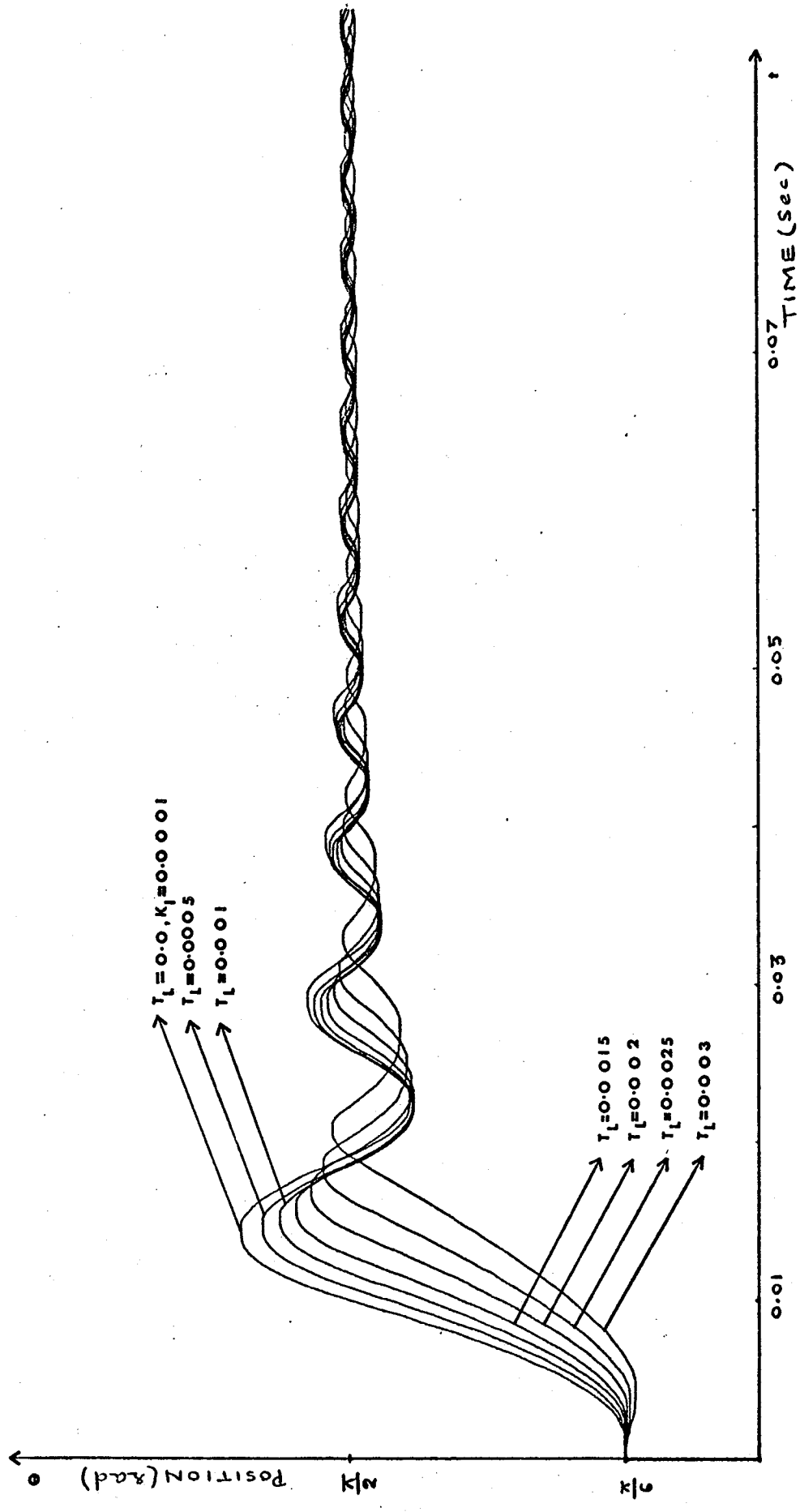

Fig.4.1.2. EFFECT OF LOAD TORQUE ON POSITION/TIME CHARACTERISTICS OF THE MOTOR

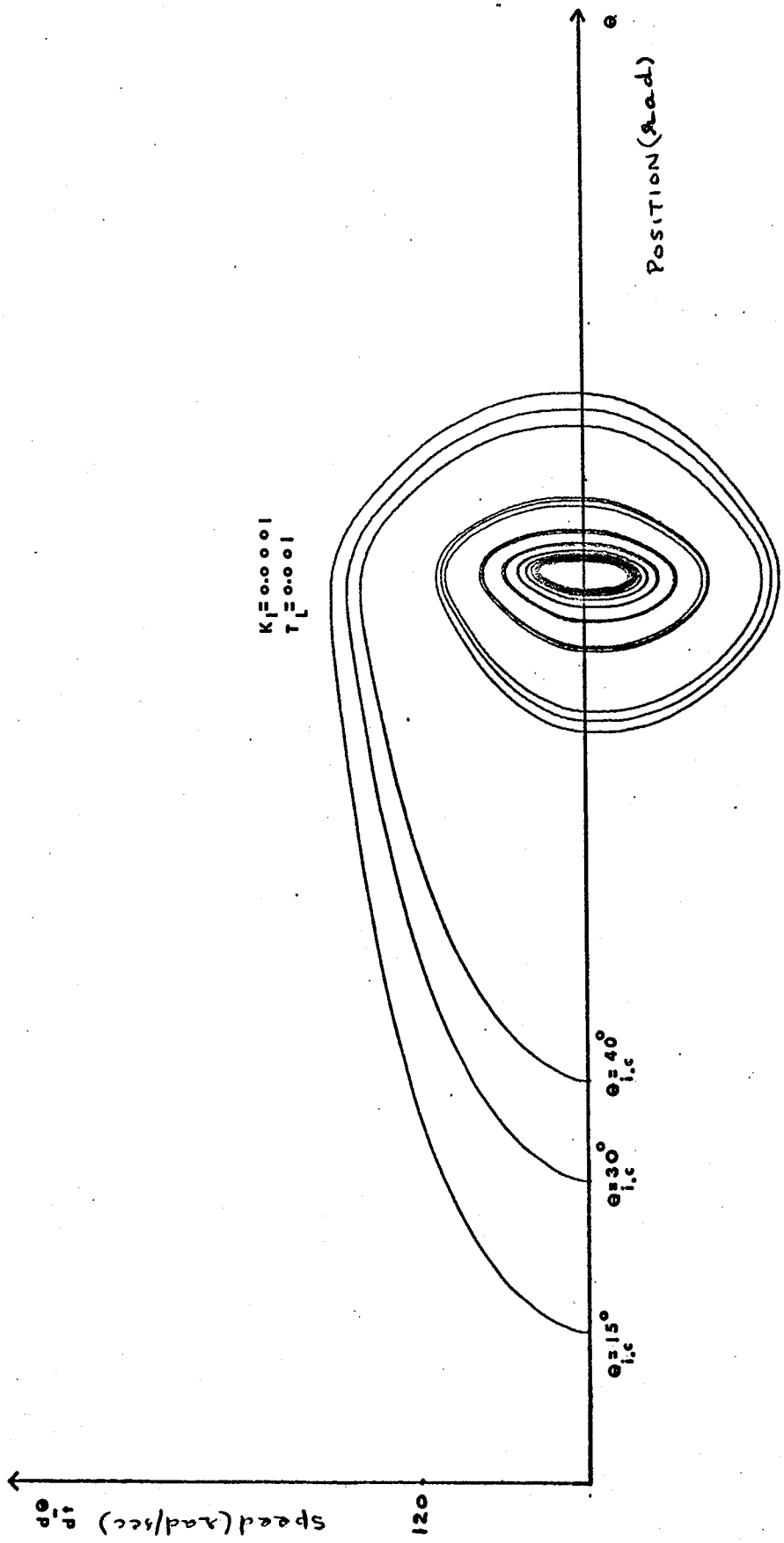

Fig.4.1.3. SPEED/POSITION CHARACTERISTICS WITH DIFFERENT STARTING POSITIONS

ating torque if the motor is started from some point before the stable starting point and vice versa if the motor is started at some point after the stable starting position. However, the minimum time taken for the execution of step angle is increased or decreased depending upon whether the motor is started from some point before the stable starting position or after it, as depicted in Fig. 4.1.4. Speed/time characteristics, for arbitrarily chosen values of load torque and damping, with different starting positions, is given in Fig. 4.1.5.

An explanation identical to the one given for position/time characteristics governing the oscillations after the motor has overshot the step angle is applicable for other characteristics too.

A comparison between the analog and digital simulation results is shown in Fig. 4.1.6.

4.2. Multi-step operation

This can be quite different from single step operation unless the motor is operated at extremely low frequency to allow the motor to settle down at the stable starting point for the next pulse. If the motor is operated at this low frequency, it will execute multi-step operation with the repitition of single-step characteristics as detailed in section 4.1. However, this is an extremely undesirable mode of operation because of comparatively longer time required by the motor to follow command pulses. Also, a considerable amount of useful torque is lost during the oscillations.

Since the stepping motor response depends basically on the frequency of input pulses, its dynamic characteristics are discussed for three different frequency regions, as follows:

First, within the low frequency region for a particular motor

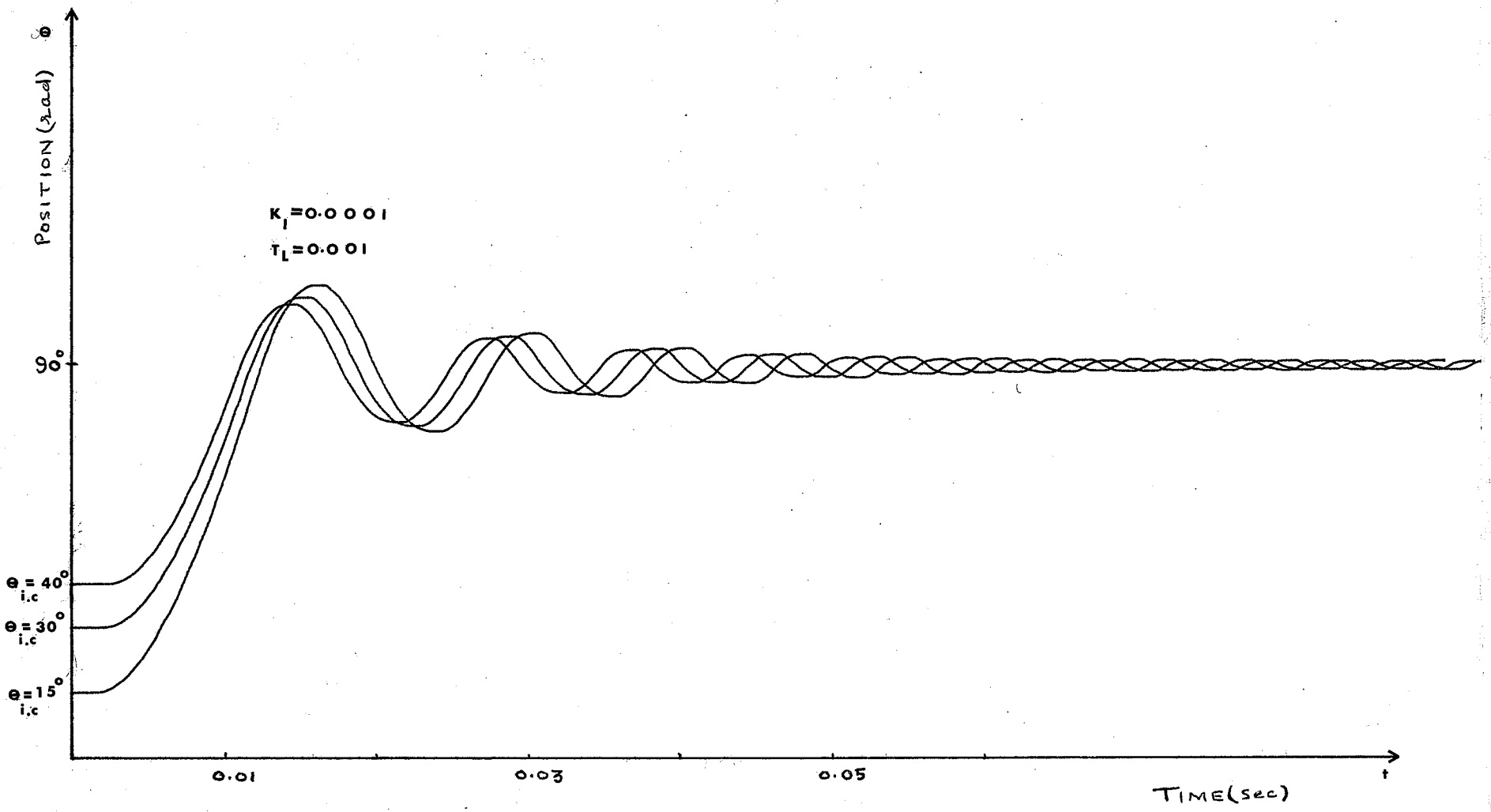

Fig.4.1.4. POSITION/TIME CHARACTERISTICS WITH DIFFERENT STARTING POSITIONS

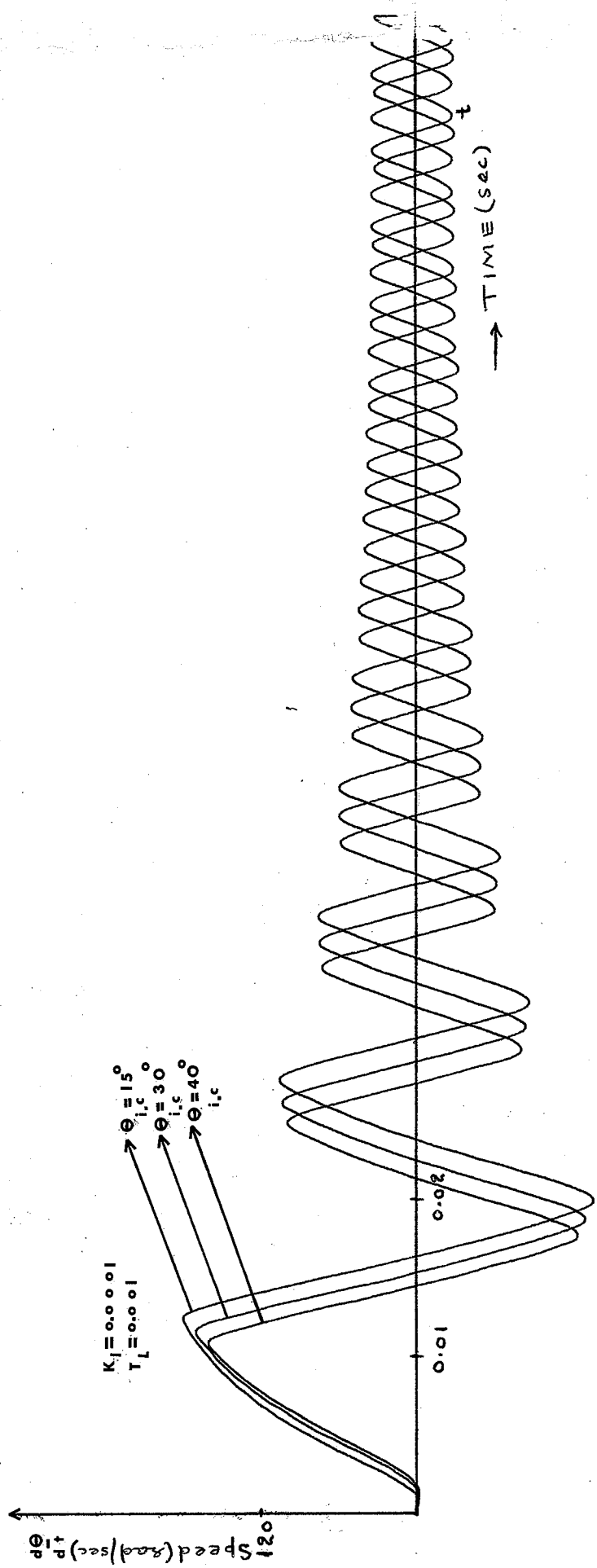

Fig.4.1.5. SPEED/TIME CHARACTERISTICS WITH DIFFERENT STARTING POSITIONS

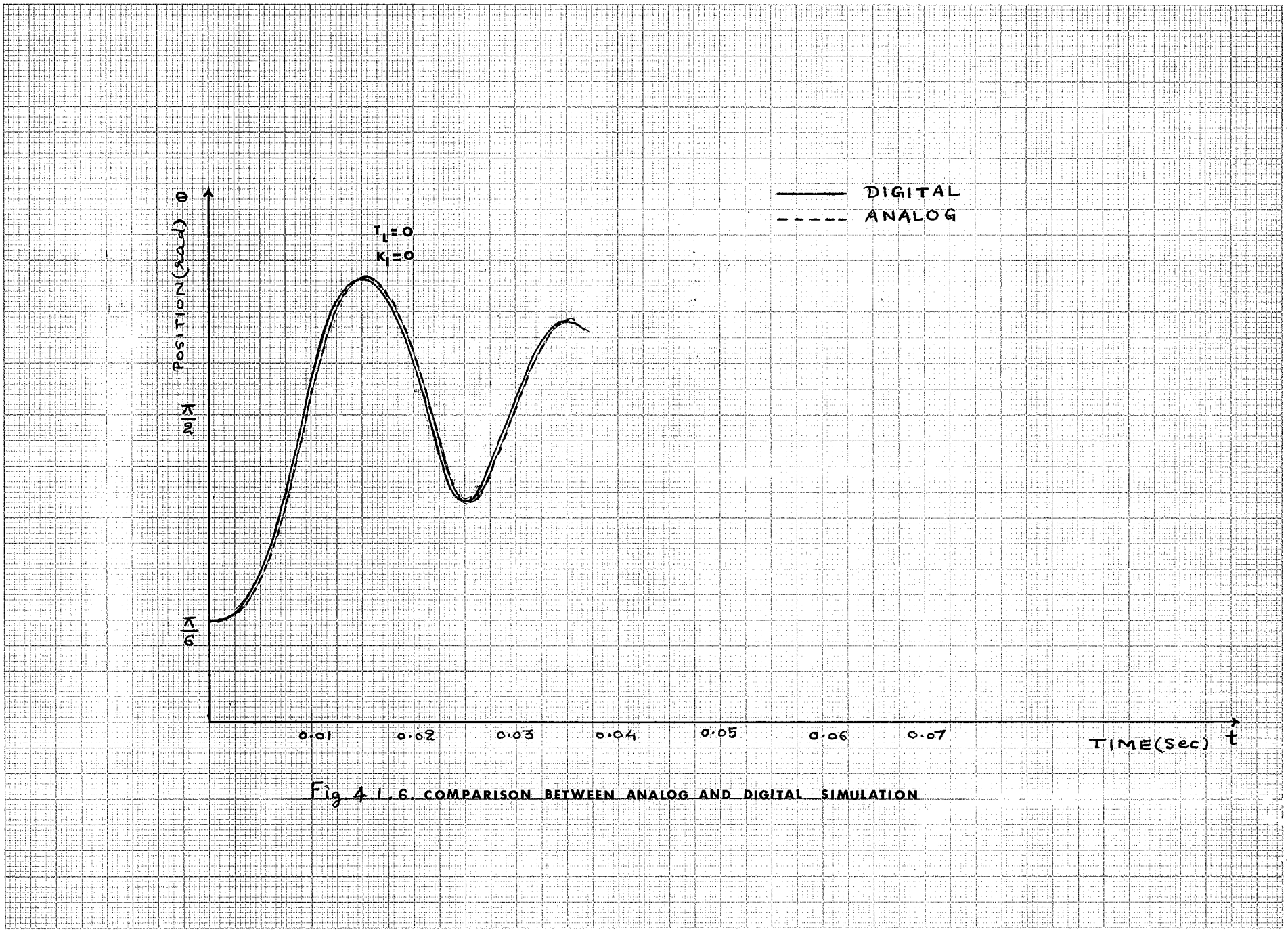

Fig. 4.1.6. COMPARISON BETWEEN ANALOG AND DIGITAL SIMULATION

(about 0 - 125 p.p.s.), the oscillations around the steps have almost been damped out. The operation in this frequency region is not critical because of the amount of overshoot or undershoot and the initial velocity at the point when next pulse is applied is pretty small. The dynamic characteristics for operation in this region are given in Fig. 4.2.1. - 4.2.3.

The second region is about 125 - 200 p.p.s. In this region, the next pulse is often applied before the response of the previous pulse has settled down. The response of the new step depends greatly on the initial value of the angle and angular velocity. For this reason, it is very possible that in some cases an incorrect motion will result. However, it is very likely that the motor will synchronize in the correct direction of rotation provided the undershoot or overshoot at a point when next pulse is applied does not exceed angle ϕ or $(\theta_s + \alpha)$ respectively, as seen from Fig. 3.1.3. The dynamic characteristics for this frequency region are given in Figures 4.2.4 - 4.2.6. It should be noticed from position/time characteristics that resonant conditions arise when an input pulse is injected into the motor before the oscillatory settling movement of the rotor resulting from the previous input pulse has had time to die away. This point of resonance is associated with the drop in torque, as shown in Fig. 4.2.7. This is because of the fact that at resonance, or during the oscillations, the rotor will, for small periods of time, try to move in the reverse direction to the general direction since the inertia of rotor will carry it past the ideal magnetic settling position and magnetic field in correcting this overshoot will try to cause the rotor to move back.

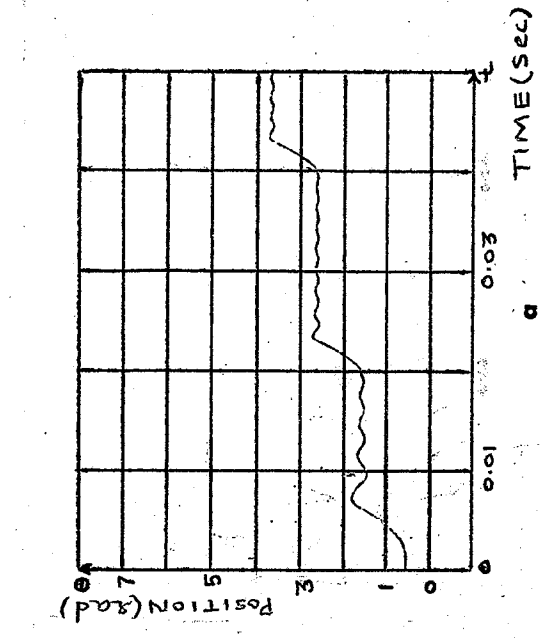

Fig.4.2.3

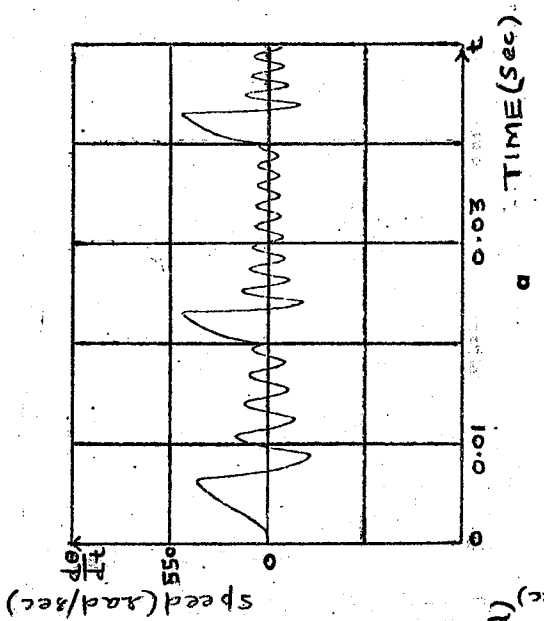

Fig.4.2.2.

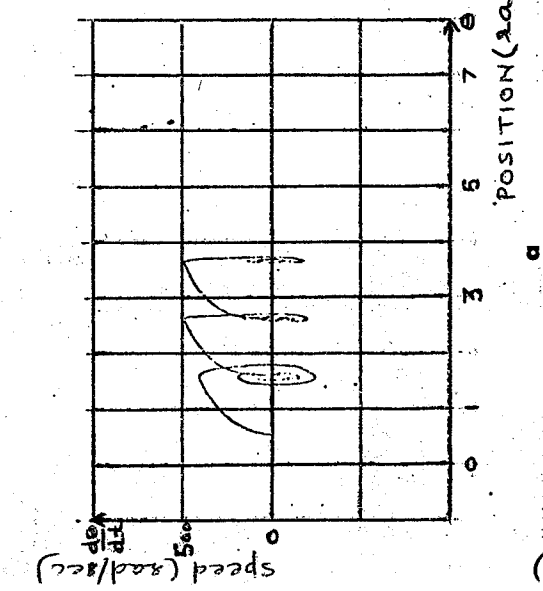

Fig.4.2.1.

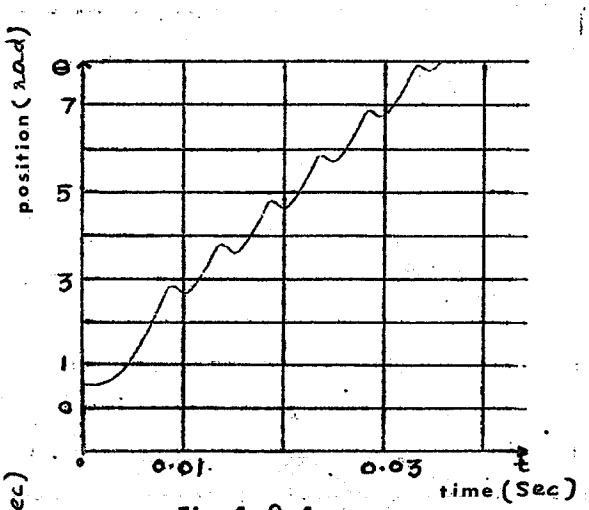

Fig.4.2.4.

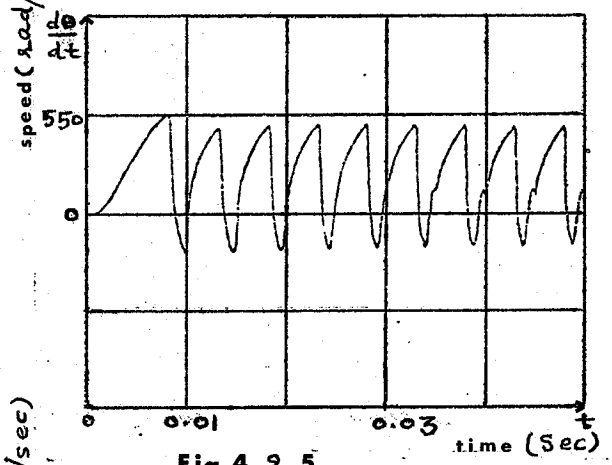

Fig.4.2.5.

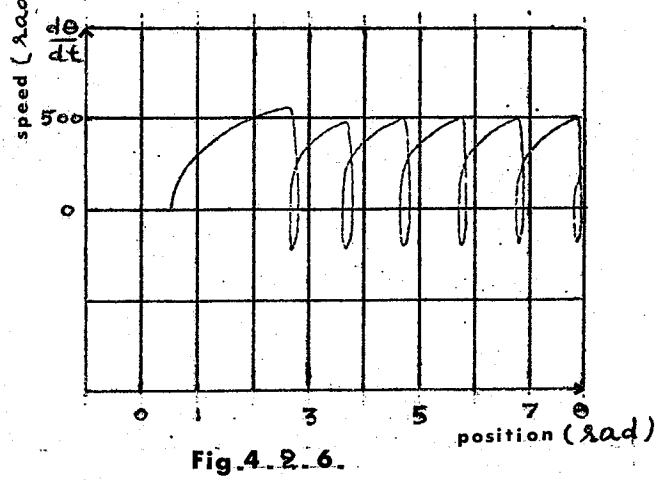

Fig.4.2.6.

PERFORMANCE CHARACTERISTICS

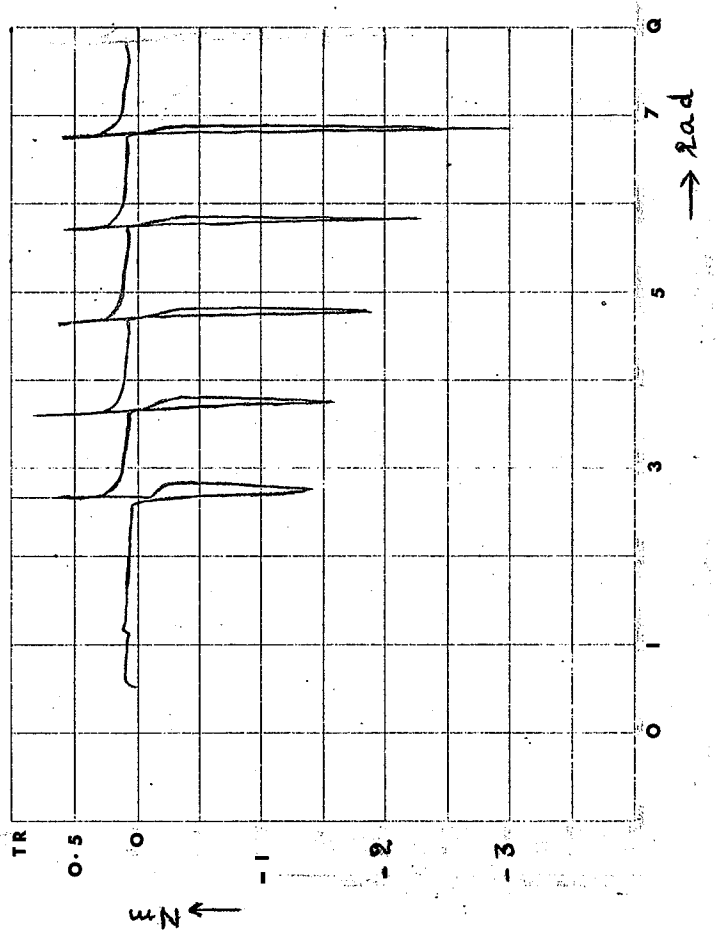

Fig.4.2.7 TORQUE/POSITION CHARACTERISTICS

Once the motor starts, it can respond to higher frequency due to the moment of inertia of the rotor. Hence it is possible for the pulse rate to be applied to the motor at lower level initially and increased subsequently until it is at maximum - operating value rate. Dynamic characteristics for this region are given in Figs. 4.2.8.- 4.2.10.

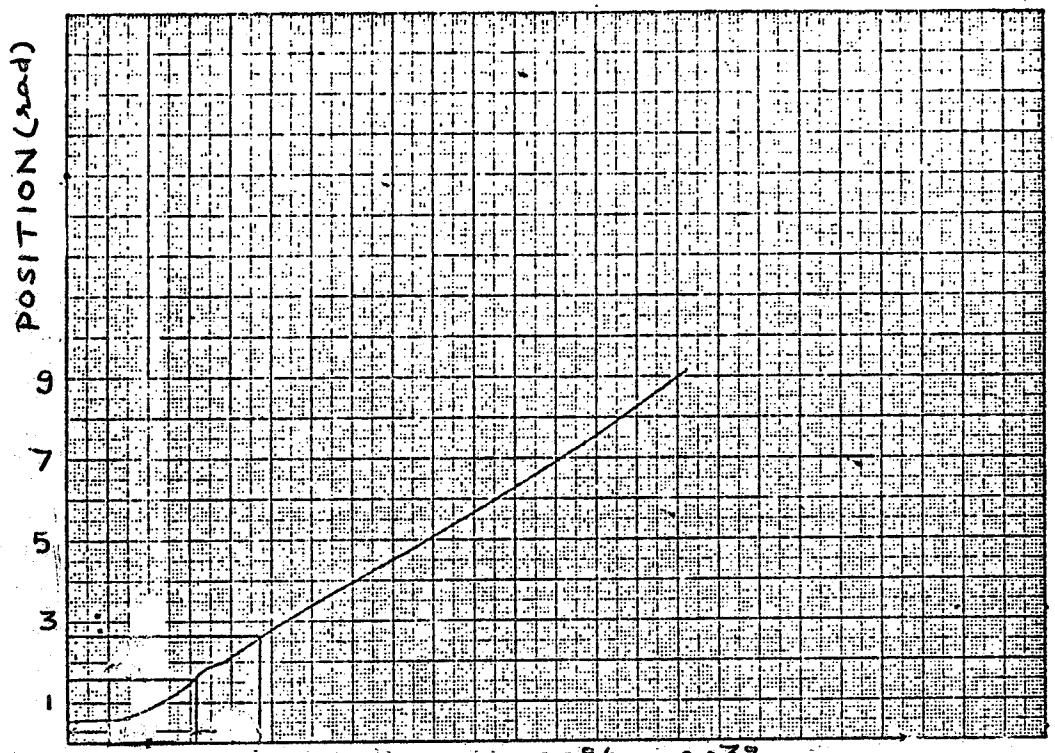

FIG. 4.2.8. POSITION/TIME

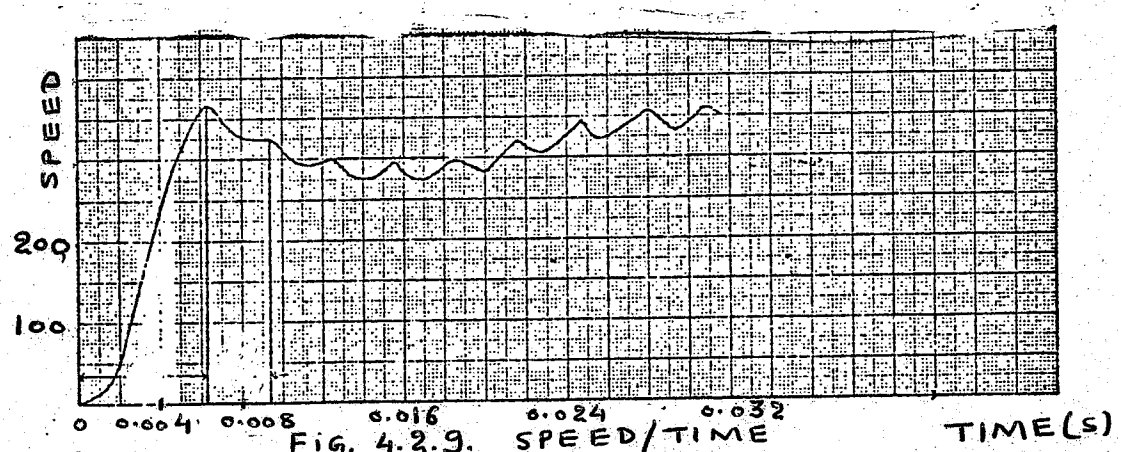

FIG. 4.2.9. SPEED/TIME

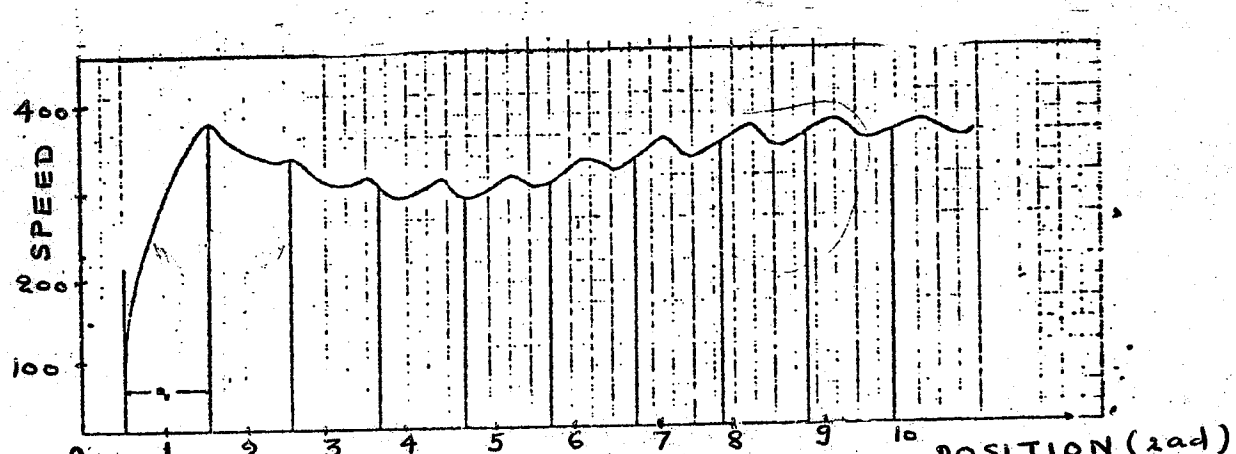

FIG. 4.2.10 SPEED/POSITION

CHAPTER 5

CONCLUSIONS

Both analog and digital models for the dynamics response of a simple three-phase variable reluctance stepping motor are developed. A generalized model for a multi-stack or multi-phase multi-teeth machine, having equal number of teeth on each stator phase and rotor is developed. Algebraic expressions for maximum pull-in frequency for single step and multistep operation are derived. Expressions for maximum operating frequency or pull-out frequency and an absolute upper limit of frequency are derived. Dynamic operating characteristics are discussed under three different frequency regions. The mathematical model developed is supported by experimentation.

This should prove valuable for both application and design engineers.

REFERENCES

1. O'Donohue, John, P., 'Transfer Function for a Stepper Motor', Control Engrg., Vol. 8, pp. 103-104, November, 1961.

2. Kuo, B.C., Singh, G., and Yackel, R., 'Modelling and Simulation of Step Motors', I.E.E.E. Trans., AC-12, pp. 745-747, 1969.

3. Venkataratnam, K., Sarkar, S.C., and Palani, S., 'Synchronizing Characteristics of a Step Motor', I.E.E.E. Trans. AC-14, pp. 510-517, 1969.

4. Robinson, D.J., and Taft, C.K., 'A Dynamic Analysis of Magnetic Stepping Motors', I.E.E.E. Trans., IECI-16, pp. 111-115, 1969.

5. Venkataratnam, K., and Mouli, M.C., 'Stability of Stepping Motors', PROC. I.E.E.E., Vol. 118, No. 6, pp. 805-812, 1971.

6. Bell, R., Loweth, A.C., and Shelley, R.B., 'The Use of Stepping Motors in Numerically Controlled Machine Tools - A Summary of the Current State of Development', Int. J. Mach. Tool Des. Res. Vol. 10, pp. 417-437, Pergamon Press, 1970.

7. Delgado, M.A., 'Mathematical Model of a Stepping Motor Operating As a Fine Postioner Around a Given Step', I.E.E.E. Trans., AC-14, pp. 394-397, 1969.

8. Goto, T., 'Dynamic Characteristics of Three-Phase Step Motors', Elect. Eng. Jap., pp. 81-92, 1964.

9. Proctor, J., 'Stepping Motors Move in' Prod. Engrg., Vol. 34, pp. 74-78, February 1963.

10. Kieburtz, R.B., 'The Step Motor - The Next Advance in Control Systems', TRANS. I.E.E.E. Autom. Control, pp. 98-103, 1964.

11. McNaught, D., and Waloff, D., 'A Review of Step Motors and Recent Developments in High Response Units', Instrum. Pract. pp. 315-322, April, 1968.

12. Thomas, A.E., Fleischauer, J., 'The Power Stepping Motor - A New Digital Actuator' Control Engng. 4, 74, (January 1957).

13. Pickup, I.E.D., Tipping, D., 'Method for Predicting the Dynamic Response of a Variable - Reluctance Stepping Motor', PROC. I.E.E., Vol. 120, No. 7.

14. Jones, C.V., 'Unified Theory of Electrical Machines', Butterworth, 1967.

15. Rummer, D.I., 'Introduction to Analog Computer Programming', New York, Holt, Rinehart and Winston, 1969.

APPENDIX 1

FOURIER SERIES FOR INDUCTANCE AND VOLTAGE WAVEFORMS

Since the waveforms for both inductances and voltages are periodic and satisfy the Dirichlet's conditions of being continuous except for the possibility of finite number of maxima and minima, these can be represented by an infinite sine and cosine series by using Fourier analysis.

If f(x) is a bounded periodic function of period 2M (i.e., f(x + 2M) = f(x)) and satisfy the above conditions, it can be represented mathematically as

$$f(x) = \frac{a_o}{2} + \sum_{n=1}^{\infty} \left(a_n \cos \frac{n\pi x}{M} + b_n \operatorname{Sin} \frac{n\pi x}{M}\right)$$

where,

$$a_n = \frac{1}{M} \int_{-M}^{M} f(x) \cos \frac{n\pi x}{M} \, dx \qquad n = 0,1,2,3,....$$

and

$$b_n = \frac{1}{m} \int_{-M}^{M} f(x) \sin \frac{n\pi x}{M} \, dx \qquad n = 0,1,2,3,....$$

Also, if the function is even (i.e., f(-x) = f(x), it will simply be

$$f(x) = \frac{a_o}{2} + \sum_{n=1}^{\infty} a_n \cos \frac{n\pi x}{M}$$

Accordingly, the values of constants a_o, a_n and b_n for the inductance and voltage waveforms for a three phase two teeth machine, as shown in Figs. 2.1.2. and 2.1.3. respectively are as follows.

(i) For the inductance waveforms

$$a_o = L_v + 2 L_{min}$$

$$a_n = \frac{2L_v}{\pi^2 n^2} \left[(-1)^n - 1\right]$$

and $b_n = o$ since it is an even function.

(ii) For the voltage waveforms

$$a_o = \frac{2}{3} V_{max}$$

$$a_n = \frac{V_{max}}{n\pi} \sin\left(\frac{2n\pi}{3}\right)$$

and

$$b_n = \frac{V_{max}}{n\pi} \left[1 - \cos\left(\frac{2n\pi}{3}\right)\right]$$

Also, the above constants for the inductance and voltage waveforms of a multiphase multiteeth VR stepping motor, as shown in Figs. 2.3.2. and 2.3.3. respectively are as follows.

(i) For the inductance waveforms

$$a_o = L_v + 2L_{min}$$

$$a_n = \frac{2L_v}{\pi^2 n^2} \left[(-1)^n - 1\right]$$

and $b_n = o$ because the function is even

(ii) For the voltage waveforms

$$a_o = \frac{2V_{max}}{P}$$

$$a_n = \frac{V_{max}}{n\pi} \sin\left(\frac{2n\pi}{P}\right)$$

and

$$b_n = \frac{V_{max}}{n\pi} \left[1 - \cos\left(\frac{2n\pi}{P}\right)\right]$$

APPENDIX 2

CHOSEN MOTOR PARAMETERS

Chosen parameters, for the the analog model of a particular motor, are given as follows:

$L_{min} = 3 \times 10^{-3}$ H

$L_v = 9 \times 10^{-3}$ H

$R = 5$ Ω

$J = 10^{-6}$ N.m. s^2/rad

APPENDIX 3

MEASUREMENT OF SELF INDUCTANCE

The method used here for the measurement of the self inductance of the stator coil was developed and used successfully by C. JONES[6], and is explained briefly as follows.

In Fig. A.3.1. L and R represent self inductance and resistance of the machine winding. R_2, R_3, R_4 are non-inductive resistances. Using a direct current source, let the current through the inductor be I, when the bridge is balanced. When the switch S is opened the current through the inductor remains instantaneously at I and subsequently drops to zero exponentially. Let ν be the instantaneous voltage across the bridge during transients. Then the instantaneous current through the lower branch will be $\nu/(R_3 + R_4)$ and instantaneous voltage across R_3 will be $[R_3/(R_3 + R_4)]\nu$. The voltage equation for the upper branch is:

$$\nu = (R + R_2)\, i + L \frac{di}{dt}$$

therefore, instantaneous current in the upper branch is

$$\frac{\nu}{R + R_2} - \frac{1}{R + R_2} L \frac{di}{dt}$$

The instantaneous voltage across R_2 will be

$$\left(\frac{R_2}{R + R_2}\right)\nu - \left(\frac{R_2}{R + R_2}\right) L \frac{di}{dt}$$

Since the bridge is balanced

$$\frac{R_3}{R_4} = \frac{R_2}{R}$$

Therefore, the voltage across the detector, the instantaneous voltage difference between voltages across R_2 and R_3, will be

$$\nu_g = - \left(\frac{R_2}{R + R_2}\right) L \frac{di}{dt}$$

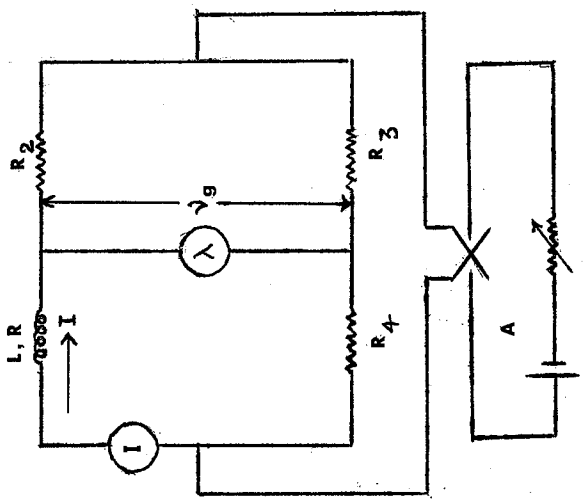

FIG.A.3.1 D.C. SELF INDUCTANCE BRIDGE

Time integral of this voltage will give

$$\lambda = \int_0^\infty V_g \, dt$$

$$= -\left(\frac{R_2}{R + R_2}\right) L \int_0^\infty \frac{di}{dt} \cdot dt$$

$$= -\left(\frac{R_2}{R + R_2}\right) L \int_I^0 dI$$

$$= \left[\frac{R_2}{R + R_2}\right] LI$$

$$\therefore \quad L = \frac{\lambda}{I} \left[\frac{R + R_2}{R_2}\right]$$

To eliminate the effect of hysteresis, switch is reversed instead of switching off. In this case

$$L = \frac{\lambda}{2I} \left[\frac{R + R_2}{R_2}\right]$$

Measurements, following the above procedure, were done on a three phase twelve teeth machine ($\theta_s = 10°$, $\alpha = 15°$) and inductance VS mechanical angle curve is shown in Fig A.3.2. This is idealized first by a triangular waveform and analyzed finally by using analysis described in Chapter 2, to get as close a curve fitting as possible, by including the required number of harmonics.

FIG. A, 3.1 SELF-INDUCTANCE/ROTOR POSITION CHARACTERISTICS